THESIS

This is to certify that the

thesis entitled

APPLICATION OF THE SHOCK RESPONSE SPECTRUM
TO PRODUCT FRAGILITY TESTING

presented by

Matthew Paul Daum

has been accepted towards fulfillment
of the requirements for

M.S. degree in Packaging

Gary Burgess
Major professor

Date 3.9.94

 MSU is an Affirmative Action/Equal Opportunity Institution

MICHIGAN STATE UNIVERSITY LIBRARIES

3 1293 01022 1913

LIBRARY
Michigan State
University

PLACE IN RETURN BOX to remove this checkout from your record.
TO AVOID FINES return on or before date due.

DATE DUE	DATE DUE	DATE DUE
	JAN 0 8 2002	
JAN 2 2 2000		
SEP 0 8 2000		

MSU Is An Affirmative Action/Equal Opportunity Institution

c:\circ\datedue.pm3-p.1

APPLICATION OF THE SHOCK RESPONSE SPECTRUM TO PRODUCT FRAGILITY TESTING

By

Matthew Paul Daum

A THESIS

Submitted to
Michigan State University
in partial fulfillment of the requirements
for the degree of

MASTER OF SCIENCE

School of Packaging

1994

ABSTRACT

APPLICATION OF THE SHOCK RESPONSE SPECTRUM
TO PRODUCT FRAGILITY TESTING

By

Matthew Paul Daum

The purpose of this study was to apply the concept of the Shock Response Spectrum (SRS) to fragility assessment. Specifically, the study addressed the appropriate procedure for the testing of products using SRS, and using SRS as an alternative to the Damage Boundary Curve (DBC) for determining product fragility. Using SRS for deflection-type failure criteria as opposed to G-level failure was also investigated, as well as the accuracy of a commercial SRS software package.

Results clearly show SRS can accurately model single degree of freedom spring/mass systems, and that the same information from a damage boundary curve can be extracted easily from a SRS plot. The lengthy and costly investment of a DBC testing procedure can be reduced to damaging only one unit in an inexpensive free fall drop test. SRS is also an accurate tool for predicting when deflection failure will occur.

Copyright by

Matthew Daum
Gary Burgess

1994

Dedicated to my loving and supportive wife, my best friend, April. Thanks for your patience these last two years.

To my Lord and Savior Jesus Christ, in whom rests all knowledge and truth.

...μυστηριου τοῦ θεοῦ και πατρος και
τοῦ χριστοῦ, εν ω εισι παντες οι
θησαυροι τῆς σοφιας και τῆς γνωσεως
αποκρυφοι.

"...the mystery of God, namely, Christ, in whom are hidden all the treasures of wisdom and knowledge." -Paul of Tarsus, circa 64 A.D.

ACKNOWLEDGEMENTS

A big thanks to Dr. Gary Burgess for his genius, patience and humor with this project.

Thank-you also to my committee members, Dr. S. Paul Singh and Dr. Bob Ofoli.

Regards to the Center for Distribution Packaging for encouraging new insights and applications in the area of packaging dynamics.

To the excellent professors at MSU who have helped shape and illuminate the field of Packaging, much thanks and appreciation.

Finally, to the many special friends in the School of Packaging who have made my graduate years enjoyable.

TABLE OF CONTENTS

LIST OF TABLES

LIST OF FIGURES

CHAPTER 1

INTRODUCTION AND LITERATURE REVIEW

1.1 INTRODUCTION

The purpose of this study was to apply the concept of the Shock Response Spectrum to fragility assessment. Specifically, the study addressed the appropriate procedure for the testing of products using SRS, and using SRS as an alternative to the Damage Boundary Curve for determining product fragility. Using SRS for deflection-type failure criteria as opposed to G-level failure was also investigated, as well as the accuracy of a commercial SRS software package.

The term shock response refers to the reaction of a single degree of freedom spring/mass system with a particular natural frequency to a single shock input. (See Figure 1). The reaction of the system is measured by the peak deceleration, G. A Shock Response Spectrum is a plot of the peak responses of different single degree of freedom systems to an input transient. Unless otherwise specified, the systems are considered to be undamped [1]. Thus, SRS is primarily concerned with the response of a system, not the characteristics of the input shock.

The fragility question to be answered is: what is it about the nature of the input shock to the product that causes it to break? To quantify this, the current accepted method is to collect experimental data and construct a damage boundary curve. This is done by subjecting the product to both short and long duration shocks, and recording the velocity change and acceleration levels that cause damage. This method can be costly and time consuming since at least two products must be damaged. Using SRS, the same information can be obtained without the need for a shock machine and damaging several units.

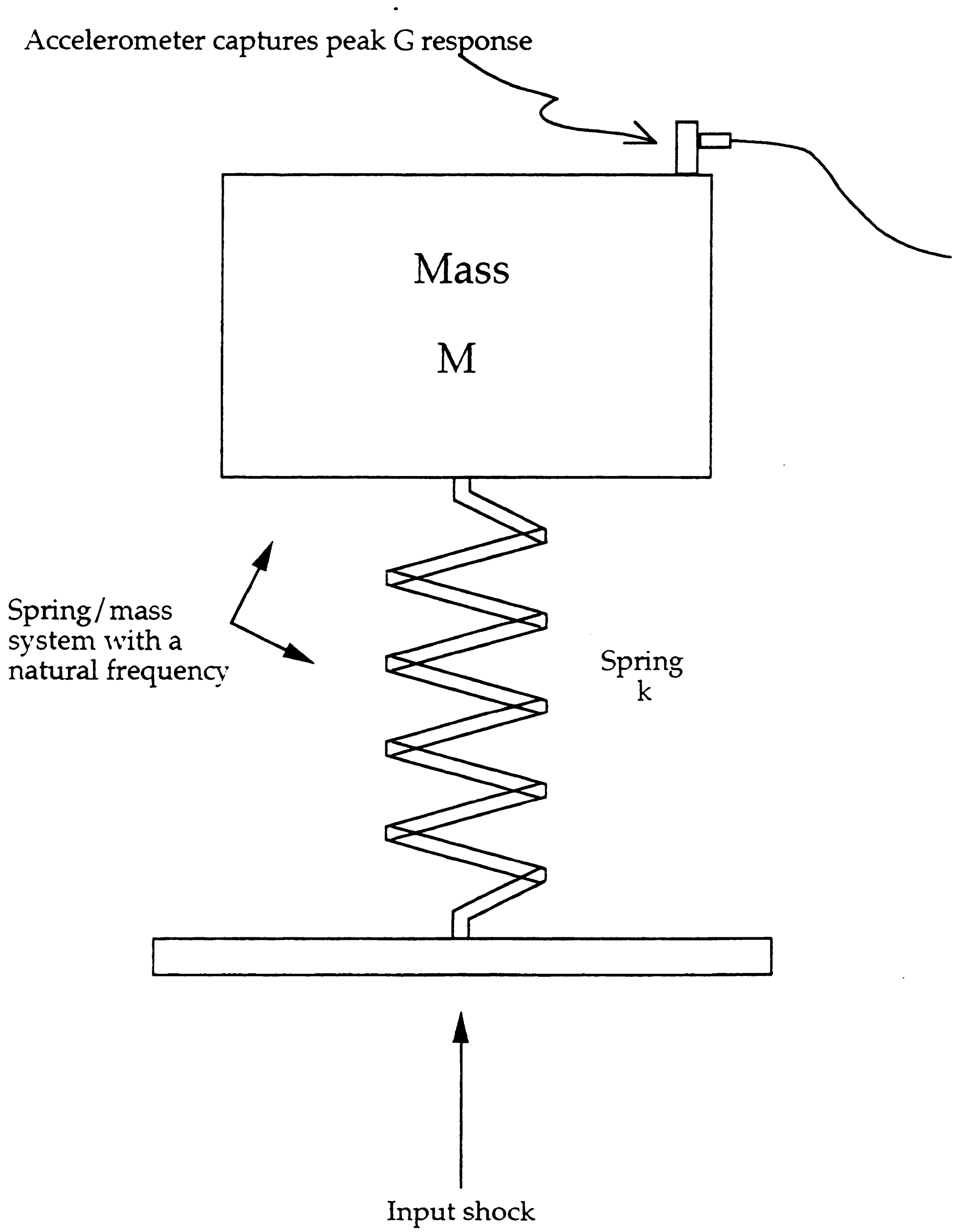

Figure 1. Response Of A Spring/Mass System With A Particular Natural Frequency To A Single Shock Input.

Traditionally for packaged products, an accelerometer is mounted to the product, usually somewhere on the base structure [2], to capture the product's response to a shock input. However, the component of a product that is the most fragile during shipping and handling is generally not what the accelerometer is mounted to. It is something else, called the "critical element". It is this component of the product that must be protected against input shocks to keep it from being damaged. The critical element must satisfy the condition of being a single degree of freedom spring/mass system in order that SRS be applicable, as will be discussed later. The traditional method begins by taking the product and its cushion and dropping it on a free-fall drop tester, recording the shock pulse. The acceleration level is then checked against the G level from a Damage Boundary Curve to predict if there is damage. The DBC test on the product really gives a picture of the fragility of the component that fails - the critical element, not the whole product. The DBC does not predict or even monitor the actual response of the element, it only describes the velocity change and G level of the input shock that caused the critical element to fail. Furthermore, DBC is specific as to what velocity change and G levels break the critical element: they are measured from a spike (produced by plastic programmers) and a square wave (produced by gas programmers). In real world testing of a product and its cushion, neither of these waveforms is reproduced. The square wave is generally considered the most damaging of waveforms [2] so the DBC can become very conservative in its fragility assessment.

The two biggest misapplications resulting from the above traditional approach are mounting the accelerometer to the product and recording the shock pulse, and trying to mount the accelerometer to the critical element itself. Mounting the accelerometer to the base of the product for example, capturing the input pulse, and then using the G level and DBC to predict damage does not take into account the actual response of the critical element. Fragility of the critical element is defined by a square wave in the DBC procedure, but actual drops are not normally square in shape, so serious overestimations of its fragility are possible. Also, without knowing the response of the critical element, using the DBC is a very indirect way of measuring fragility, since it is not the product's shell (or whatever else the accelerometer is mounted to) that is damaged, but a component inside it. The actual response of the critical element is completely ignored.

Mounting the accelerometer to the critical element to measure its response is also ineffective for several reasons. First, the critical element may be too small for an accelerometer, like the filament of a light bulb. Another problem may be the location of the critical element; for instance, how does one attach an accelerometer to the magnetic head of a hard drive? Finally, by attaching the accelerometer to the critical element, the mass will necessarily change, causing a change in the behavior of the critical element. Even if the response can be accurately measured, comparing it to the DBC is not a correct application, since the DBC describes the shock input, not the critical element's response.

A problem with capturing response pulses in general is the presence of other components in the product that were not meant to be monitored. And since there are many other components present in a product besides the critical element, each vibrating at different natural frequencies which the accelerometer can detect, filtering the pulse to eliminate "ringing" is necessary. Without filtering, ringing (undesirable motion superimposed on the original waveform) may cause the data to appear to have false peak accelerations, inaccurate velocity changes and false coefficients of restitution. Using SRS would eliminate the need for filtering, since filtering has virtually no effect on SRS plots, except when the natural frequency of the element matches the ringing [3,4]. Using SRS would also eliminate the ambiguity in the DBC, since capturing the input shock and knowing the natural frequency of the critical element is all that is necessary to predict whether there will be failure or not. There is no need to mount an accelerometer to the critical element, since its response can be accurately calculated by SRS. In other words, SRS eliminates the need to capture the element's response, since the response can be calculated from the input shock. This significantly reduces the worries of filtering. SRS also gives a much truer picture of fragility of the critical element, since it is not dependent on or derived from a spike or square wave.

Since SRS is concerned with a critical element's response to a shock, not the input shock itself, any shape input shock pulse can be used so long as it damages the critical element. This is not true with damage boundary curves: the input shock used to damage the product must be a square wave, or a half sine wave. With SRS, a free fall drop tester could be used, moving the height up in some reasonable increments until damage has occurred, and analyzing that input pulse using SRS to predict the peak G of the critical element. From the peak G predicted by SRS, a damage boundary curve could also be constructed. This would eliminate the need for an expensive shock table, and reduce the number of units required to construct a damage boundary curve, saving money and time.

There are times when failure will occur due to the deflection of a component, not the shock it receives. A component within a product may fail, for example, because it deflects to the point where it bumps into something else. SRS could be used to predict the maximum allowable deflection, and the G level that causes the critical deflection.

Finally, since damage boundary is a very conservative approach to assessing fragility, SRS could reduce the amount of cushioning for packages [5].

1.2 LITERATURE REVIEW

The Shock Response Spectrum (SRS) has been known and used in the scientific community for many decades [6]. SRS was first used as a tool for determining the resistance of buildings to earthquakes [1,6]. Since then, methods to calculate SRS have been developed and applications sought in several fields [7,8,9,10,11]. Uses have been identified for the standardization of shock machines, and making direct response-based correlations between product fragility and a package drop test [3,12]. Several authors have outlined the basics behind SRS analysis [7,11,12,13], while pointing out its virtues as a design tool and as a shock test control parameter [3,6]. Little application has been made directly to the field of packaging, however, particularly its use as a testing alternative to the Damage Boundary Curve (DBC). A study by Robert E. Newton has recognized and outlined the relationship between the DBC and Shock Response Spectrum, namely how the DBC is derived from the basic premises of the Shock Response Spectrum [14].

CHAPTER 2

THEORETICAL DEVELOPMENT

2.1 SRS THEORY

For any particular input pulse, the theoretical response of an undamped, single degree of freedom spring/mass system with a particular natural frequency can be calculated using Newton's laws of motion. The peak acceleration response of a spring/mass system is a function of its natural frequency. A plot of peak deceleration versus natural frequency is called the Shock Response Spectrum. For an ideal undamped spring/mass system, the SRS plot is determined by applying Newton's laws of motion to the situation in Figure 2.

From Newton's law, Force = Mass x Acceleration

$$k(x - y) = m \frac{d^2y}{dt^2} \qquad \text{Eq. 1.}$$

where:

k = spring constant for a linear spring

m = mass

y(t) = response position at any instant measured from the static equilibrium position

x(t) =prescribed base position at any instant measured

t = time

(x - y) = relative displacement

This is a second order ordinary linear differential equation in the unknown function of time y(t). For no motion of the base (x = 0), the system executes free vibration and the solution is [16]:

$$y = C_1 \sin \omega t + C_2 \cos \omega t \qquad \text{Eq. 2.}$$

where C_1 and C_2 are constants determined by the starting positions and velocities, and ω is related to the natural frequency of vibration through [9]

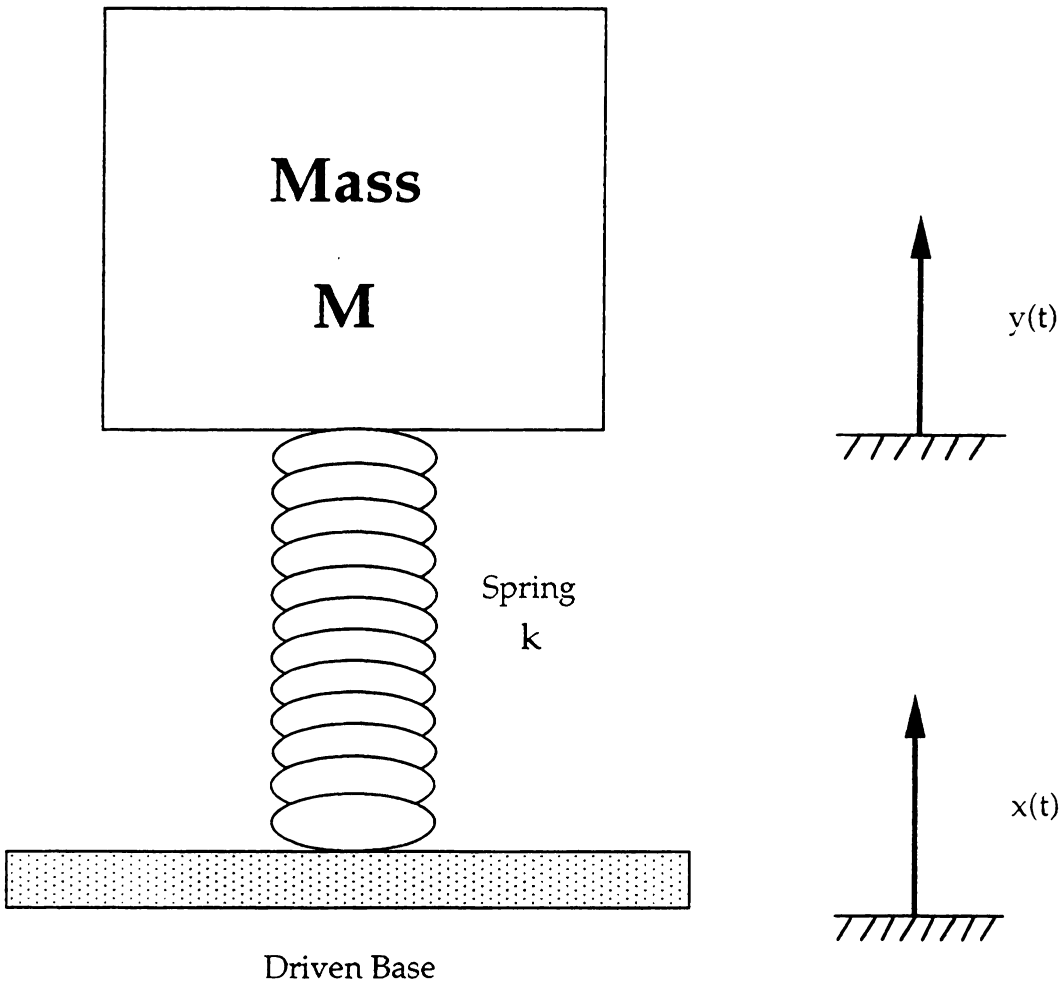

Figure 2. Newton's Law Of Motion Can Be Used To Determine The Response Of A Mass To A Particular Excitation.

$$\omega = 2\pi f_n$$

$$f_n = \frac{1}{2\pi}\sqrt{\frac{kg}{W}}$$

$$W = mg$$

$$g = \text{acceleration due to gravity } (386.4 \text{ in / sec}^2)$$

For a prescribed motion of the base, the system executes forced vibration and the solution is [16]:

$$y = C_1 \sin \omega t + C_2 \cos \omega t + \omega \int_0^t x(s) \sin \omega (t - s) ds \qquad \text{Eq. 3.}$$

Applying the starting conditions that y and $\frac{dy}{dt}$ are both zero at t = 0 (mass is at rest initially) gives $C_1 = C_2 = 0$.

This solution is not very useful in its present form because it relates positions to each other: what is needed for SRS is to relate accelerations to each other. This is easily accomplished by first differentiating this equation twice to obtain $\frac{d^2y}{dt^2}$ and then using integration by parts [16] along with the initial conditions x = $\frac{dx}{dt}$ = 0 at t = 0. The result is:

$$\frac{d^2y}{dt^2} = \omega \left[\sin(\omega t) \cdot \int_0^t \frac{d^2x}{dt^2} \cos(\omega t) dt - \cos(\omega t) \cdot \int_0^t \frac{d^2x}{dt^2} \sin(\omega t) dt \right] \qquad \text{Eq. 4.}$$

where: $\frac{d^2y}{dt^2}$ = the response acceleration at any instant

$\frac{d^2x}{dt^2}$ = the input acceleration at any instant (known)

Equation 4 is the governing equation for finding the peak acceleration response of an ideal undamped spring/mass system to any input shock pulse.

There are two important parts to the response acceleration which can be obtained using this equation. These two parts are for t < T and for t > T, where T is the duration of the input shock. The response during the input shock (t < T) is known as the primary response, and the response after the input shock (t > T) is called the residual response. The peak response acceleration during the primary and residual responses will be evaluated and compared: the larger of the two is used for the SRS.

There are two important types of input shock pulses for which the response of a single degree of freedom spring/mass system can be evaluated exactly. The first is a short duration pulse, (or spike), such as that obtained using the plastic programmers on a shock table. See Figure 3. If the input shock is very short in duration compared to the natural period of vibration ($\frac{1}{f_n}$) of the spring/mass system, then $\frac{d^2x}{dt^2}$ in the integral is non-zero only for a very short time period around t = 0. This means that $\cos\omega t$ and $\sin\omega t$ are essentially 1 and 0 respectively. Therefore:

$$\frac{d^2y}{dt^2} = \omega\left[\sin\omega t \cdot \int_0^t \frac{d^2x}{dt^2} \cdot 1dt - \cos\omega t \cdot \int_0^t \frac{d^2x}{dt^2} \cdot 0dt\right] \qquad \text{Eq. 5.}$$

$$= \omega \cdot \sin\omega t \cdot \Delta V \qquad \text{Eq. 6.}$$

The term $\int_0^t \frac{d^2x}{dt^2} \cdot 1dt$, which represents the area under the acceleration versus time curve, is just the velocity change, ΔV, for the input shock. The peak response occurs when $\sin(2\omega t)$ is equal to 1. Using $\omega = 2\pi f_n$ and reporting the peak response in G's = $\frac{d^2y}{dt^2}/g$,

$$\text{peak response G} = \frac{2\pi f_n \Delta V}{g}. \qquad \text{Eq. 7.}$$

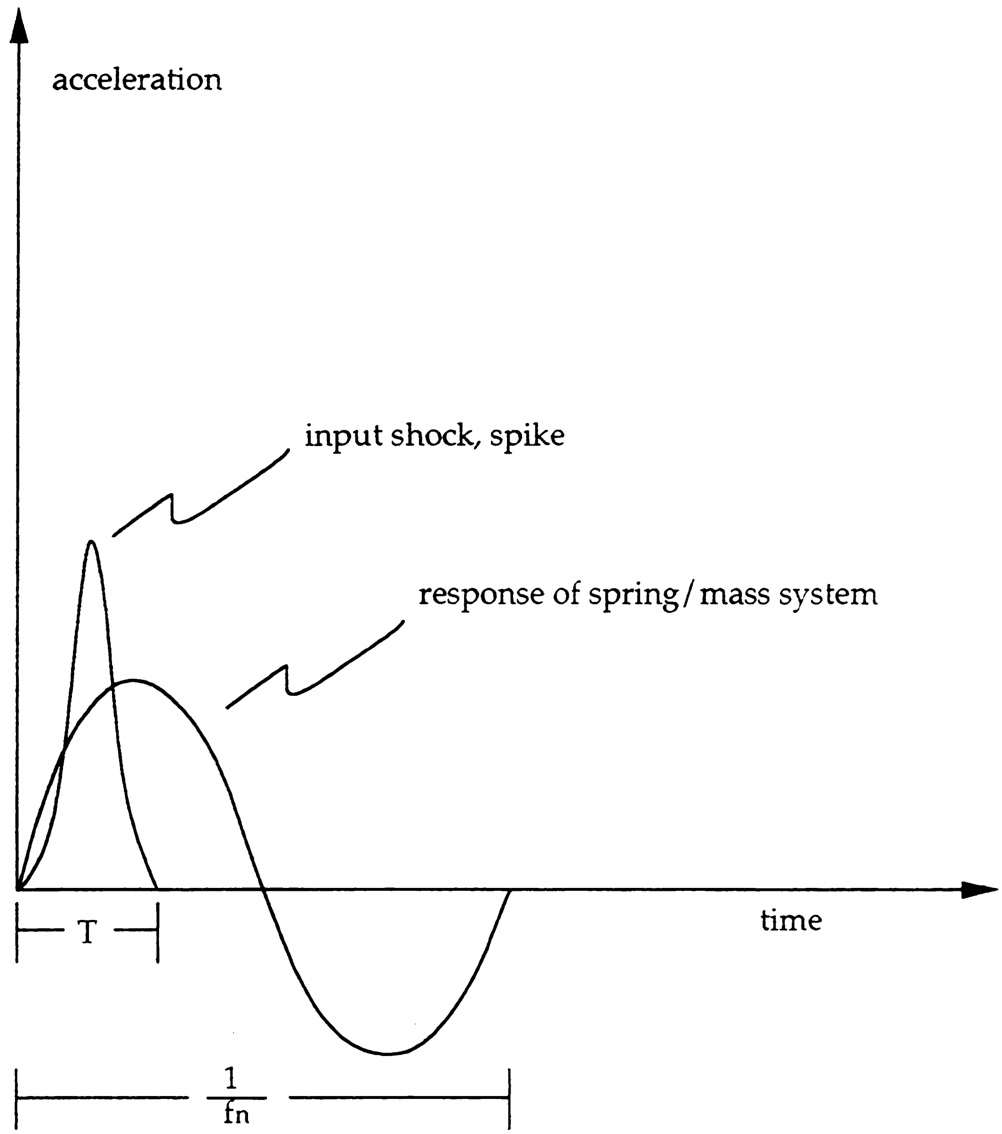

Figure 3. Input Shock And Response Of A Spring/Mass System

This says the response of any spring/mass system to a spike does not depend on the peak acceleration or the duration of the spike, but only on the velocity change of the spike. This also says that the response G is proportional to the natural frequency of the spring/mass system for a spike. Since an SRS plot is a plot of peak response G versus natural frequency of a spring/mass system, the SRS plot for a spike begins as a straight line with a slope of $(2\pi\Delta V)/g$, as shown in Figure 4. In fact, all SRS plots must start out as straight lines. This is true because as the SRS plot starts out, the natural frequencies are low and so the period $\frac{1}{f_n}$ will always be large compared to the duration of the input shock. When the natural period of vibration is not sufficiently larger than the duration of the input shock, the linear relationship between G and natural frequency does not hold true. The response must then be determined by evaluating Equation 4. The linearity of SRS plots as they start out is one feature which can be used to check the accuracy of commercial software.

The second important type of input shock pulse for which the response can be evaluated exactly is a square wave pulse, such as that obtained using the gas programmers on a shock table. In this case, $\frac{d^2x}{dt^2}$ = A = constant for the duration T of the pulse as shown in Figure 5. Two separate times of the input shock must be evaluated, the input shock during duration T, and the input shock after T. The response to the input shock during duration T is known as the primary response, and the response to the input shock after T is known as the residual response.

Let A = $\frac{d^2x}{dt^2}$ = input acceleration.

The primary response then is:

$$\frac{d^2y}{dt^2} = \omega\left[\sin(\omega t)\cdot\frac{A}{\omega}\sin\omega t - \cos\omega t\cdot\frac{A}{\omega}(1-\cos\omega t)\right] \qquad \text{Eq. 8.}$$

Evaluation of SRS Software
C:\TP2\DATA\MPD\BRES1.PL2

10:30:11 PM
04-29-1993

	Channel 1	Channel 2
SRS Type:	Composite	
Resolution:	20	PPO
Damping:	0.00	
Peak Acc:	195.91	G's
Peak Fn:	278.58	Hz
Min Acc:	-193.36	G's
Min Fn:	251.07	Hz

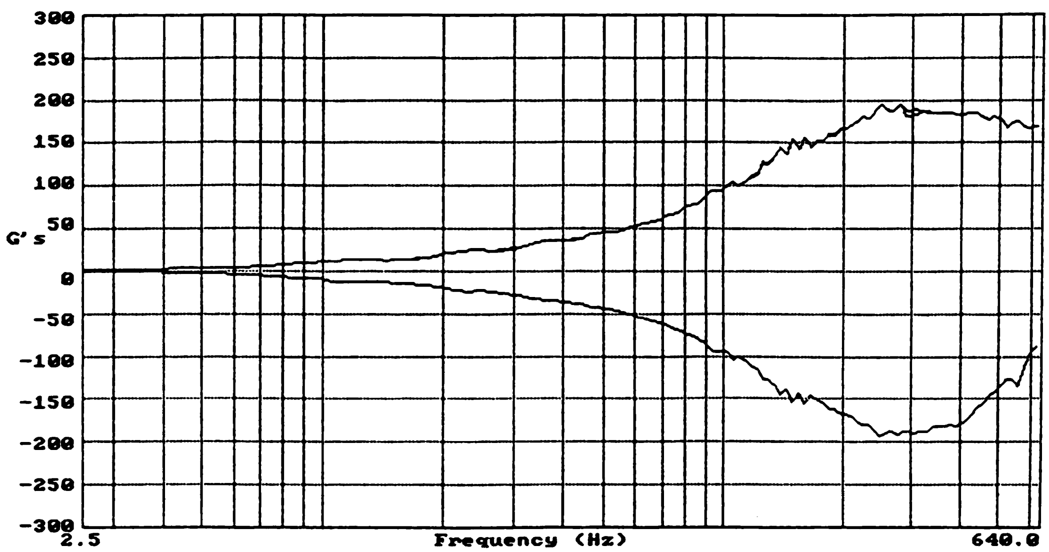

Notes: Top line is maximum response
Bottom line is max minimum response

Michigan State University

TEST PARTNER

Figure 4. Typical SRS Plot For a Spike.

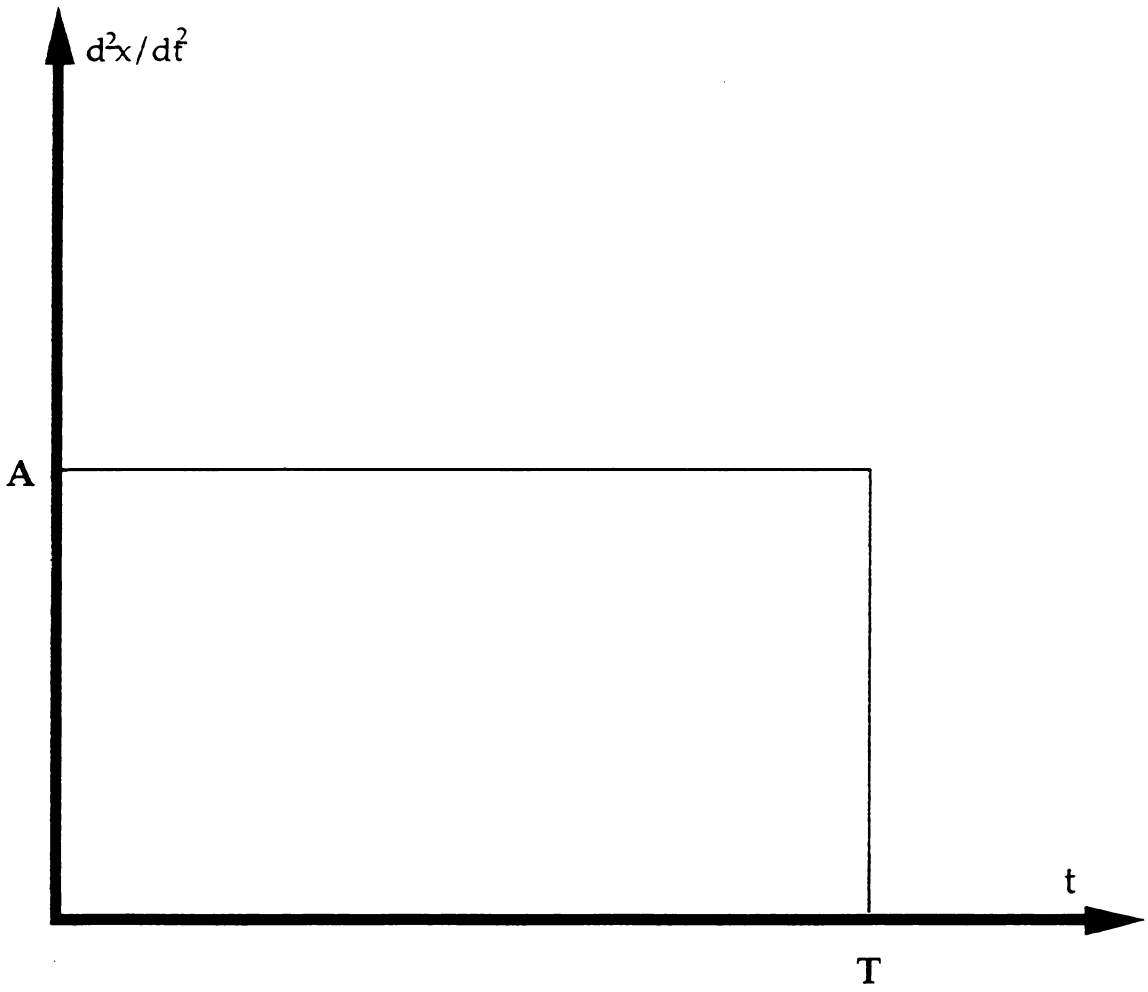

Figure 5. Ideal Square Wave Input.

or: $$\frac{d^2y}{dt^2} = A[1 - \cos\omega t] \qquad \text{Eq. 9.}$$

Dividing by g to obtain G's:

$$\text{Gresponse} = \text{Ginput}[1 - \cos 2\pi f_n t] \text{ for } t < T \qquad \text{Eq. 10.}$$

It is important to note that this is only the primary response. This is valid only when the time t chosen is less than the duration T of the square wave. The residual response occurs after the duration T of the input shock. Since the input acceleration is discontinuous, two separate integrals must be evaluated. From Equation 4,

$$\int_0^t = \int_0^T + \int_T^t \qquad \text{Eq. 11.}$$

Part 1. $$\int_0^T A\cos(\omega t)dt = \frac{A}{\omega}\sin\omega T \qquad \text{Eq. 12.}$$

$$\int_0^T A\sin(\omega t)dt = \frac{A}{\omega}(1 - \cos\omega T) \qquad \text{Eq. 13.}$$

Part 2. $$\int_T^t = 0 \text{ because } \frac{d^2x}{dt^2} = 0 \text{ for } t > T \qquad \text{Eq. 14.}$$

The response then becomes:

$$\frac{d^2y}{dt^2} = \omega\left[\sin(\omega t)\cdot\frac{A}{\omega}\sin(\omega T) - \cos\omega t\cdot\frac{A}{\omega}(1 - \cos\omega T)\right]. \qquad \text{Eq. 15.}$$

or:

$$\text{Gresponse} = \text{Ginput}[\cos\omega(t - T) - \cos\omega t] \text{ when } t > T. \qquad \text{Eq. 16.}$$

This is the residual response.

Therefore, if $T < \frac{1}{2f_n}$, the peak primary response according to Equation 10 will be:

$$\text{peak response G} = G_{in}\left[1-\cos\left(2\pi f_n T\right)\right] \qquad \text{Eq. 17.}$$

And if $T \geq \frac{1}{2f_n}$, the peak response G will be:

$$\text{peak response G} = 2G_{input}. \qquad \text{Eq. 18.}$$

The peak residual response for either $T < \frac{1}{2f_n}$ or $T \geq \frac{1}{2f_n}$ can be determined using Equation 16 (see Appendix A). By differentiating with respect to t to find the maximum, the result is:

$$\text{peak residual response G} = G_{in}\sqrt{2(1-\cos\omega T)} \qquad \text{Eq. 19.}$$

In summary, for square waves, if $T \geq \frac{1}{2f_n}$, then:

1) The peak G will be $2G_{input}$.
2) The peak G will occur during the input shock.
3) The peak residual response will be $G_{in}\sqrt{2\left(1-\cos 2\pi f_n T\right)} < 2G_{in}$.

And if $T < \frac{1}{2f_n}$, then:

1) Peak G will be $G_{in}\sqrt{2\left(1-\cos 2\pi f_n T\right)} < 2G_{in}$.
2) Peak G will occur after the input shock.
3) The peak G during the input shock will be $G_{in}\left(1-\cos 2\pi f_n T\right)$.

Therefore, all SRS plots for ideal square waves will be as shown in Figure 6.

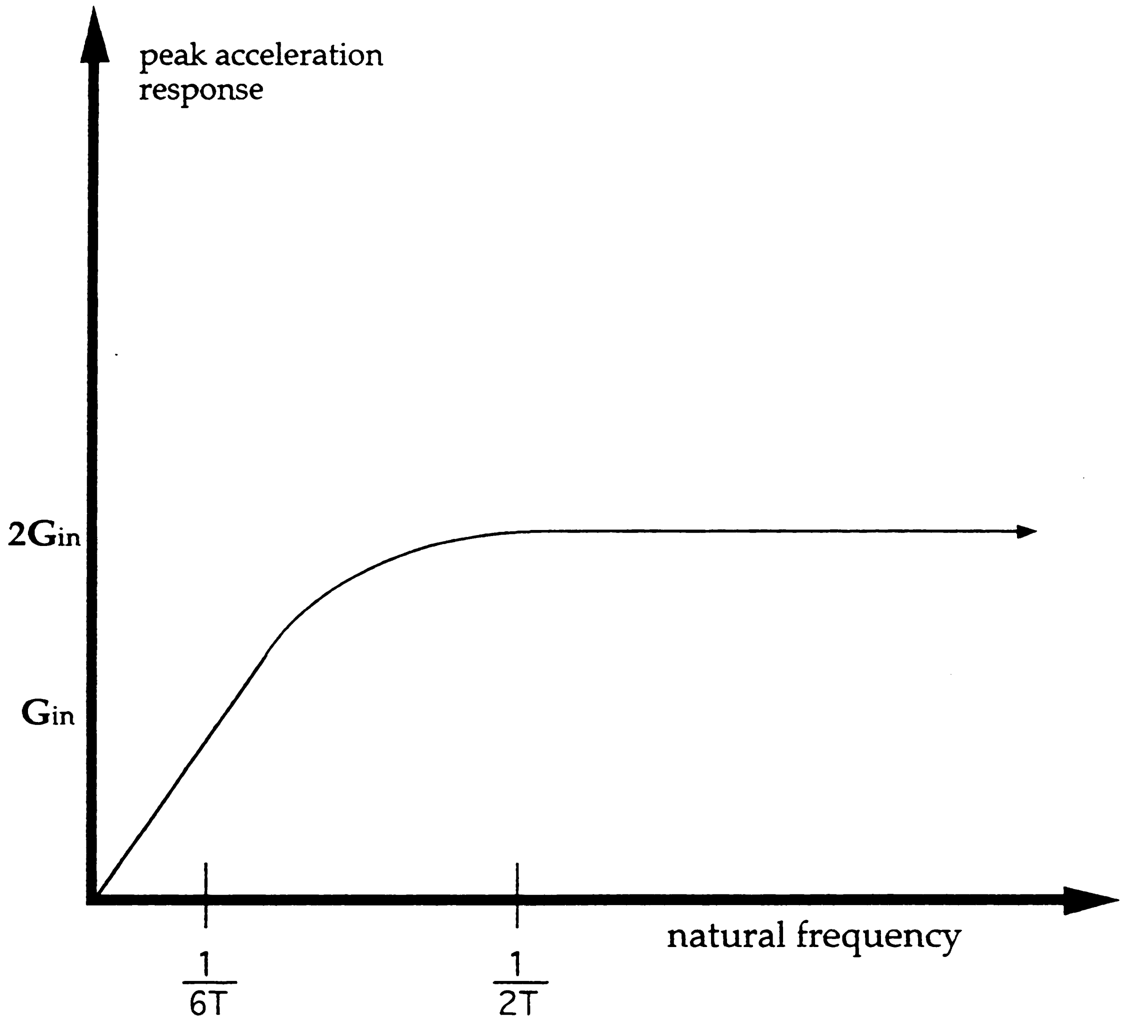

Figure 6. SRS Plot For An Ideal Square Wave Input.

To relate displacement failure to SRS, simply rearrange Equation 1, and divide by acceleration, g, to obtain:

$$G = (2\pi f_n)^2 \frac{d}{g} \qquad \text{Eq. 20.}$$

where: G = maximum acceleration from an SRS plot at f_n

d = distance between the mass and base structure.

If the maximum allowable displacement is known, Equation 20 gives the acceleration response for when the critical deflection is reached. Therefore, performing SRS on an input shock will tell the user how far the component will deflect in response to that shock.

2.2 RELATIONSHIP BETWEEN DAMAGE BOUNDARY AND SRS

The conventional approach to fragility testing is a method called the Damage Boundary Curve (DBC). The DBC is essentially a two dimensional index of fragility that takes into account both the amplitude and duration of the shock. The DBC presumes that only two aspects of an input shock pulse to a product are related to damage: the peak G and the velocity change (area under the acceleration versus time waveform). The DBC relates peak G on the vertical axis to the total velocity change (ΔV) on the horizontal axis to product damage [15]. The development of a damage boundary curve for a product is presented in full in ASTM D 3332-77 (1983) "Standard Test Methods for Mechanical Shock Fragility of Products Using Shock Machines" [2]. The following is a brief summary of some of the important steps in conducting a damage boundary test.

The first step is to determine the critical velocity change (ΔV_{cr}) for a product. This is done using the plastic programmers on a shock machine, which produce short duration (about two milliseconds) half-sine shocks. Affixing the product to the table, the table is raised and dropped from a series of heights in slightly increasing increments until the product is damaged. The last drop that causes damage is used to determine the product's critical velocity change.

The second step is to determine the critical acceleration for the product. This is accomplished using the gas programmers on the shock table. Gas programmers use gas compressed in a piston as the contact surface to generate a trapezoidal pulse. High gas pressures produce short trapezoidal pulses with high acceleration levels, and low gas pressures produce long duration, low acceleration pulses. It is important to note the desired pulse is a perfectly square waveform, but an instantaneous rise time is impossible to produce in a commercial setting. The trapezoid pulse has a very fast (not instantaneous) rise time, and is a close approximation. The table drop height used in this part of the test must be chosen to produce a table velocity change of at least: [($\pi/2$) x (critical velocity change obtained using the plastic programmers)]. To begin this phase of the testing, a second product is affixed to the table and dropped onto the gas programmers. The gas pressure in the cylinder is then increased while the drop height is held constant: this increases the acceleration level while keeping velocity change the same. This pressure is gradually increased until damage occurs. The last drop that causes damage is the product's critical acceleration.

The fragility picture for this particular product is now constructed using the product's critical velocity change and critical acceleration as shown in Figure 7. The resulting plot is able to show the relationship between the critical velocity change and critical acceleration of an input pulse, and damage to the product for which that DBC was constructed. Any input shock pulse with $\Delta V > \Delta V_{cr}$ and $G > G_{cr}$ will result in damage. A pulse with $\Delta V > \Delta V_{cr}$ but $G < G_{cr}$ will in theory not cause damage. The same can be said of a pulse that has $\Delta V < \Delta V_{cr}$ and $G > G_{cr}$.

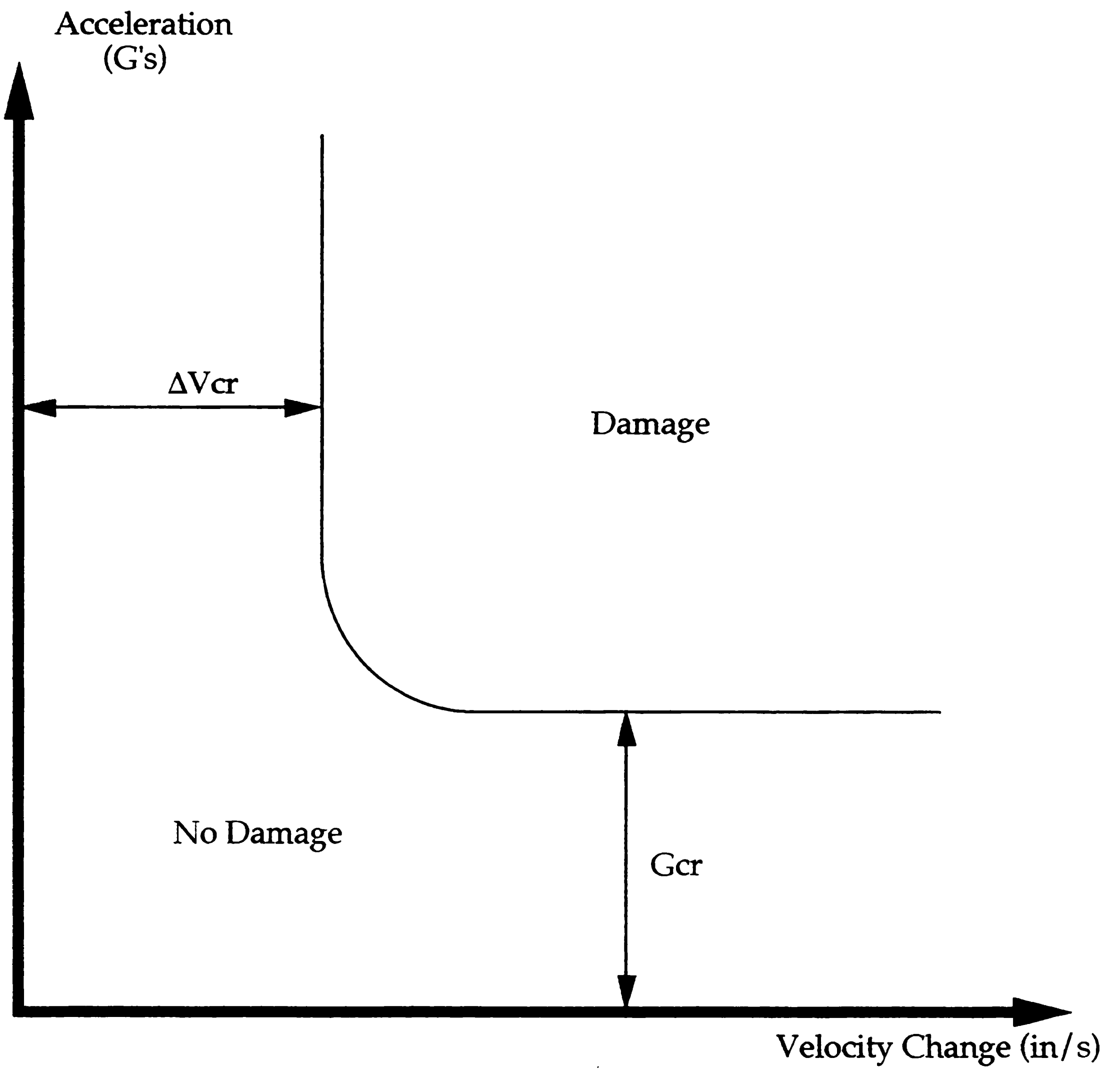

Figure 7. Relationship Between Damage Boundary And Results From SRS.

An important point to the above process is the fact that the DBC generated is valid only for one orientation of the product. A product the shape of a cube would require six DBC's to represent the overall fragility of the product. This can obviously become a time consuming and expensive undertaking.

The reason that the DBC in Figure 7 has the shape it does is that it is based on an idealized model of the product. See Figure 8. Note the component called the "critical element." The critical element can be any component which must not be damaged, and that meets the following criteria:

1) The critical element must behave like a spring/mass system.

2) The critical element in question must be the thing that breaks during both the plastic and gas programmer shocks.

Using the results from the spike and square wave shocks from SRS, a correlation can now be made to the damage boundary curve. Recall that the damage boundary curve attempts to answer what it is about the nature of the input shock to the product that causes damage to the critical element. It answers the question by identifying a critical velocity change and a critical acceleration, both of which must be satisfied for failure to occur. To relate the experimental results, ΔV_{cr} and G_{cr}, to the nature of the critical element, two results from SRS are applicable. The first is the input shock from the plastic programmers which is essentially a spike, for which the peak response of the critical element is given by Equation 7. Since by assumption the critical element breaks when $G = G_{ce}$ where G_{ce} is the fragility of the critical element and f_n is its natural frequency, this predicts that

$$\Delta V_{cr} = \frac{G_{ce} g}{2\pi f_n} \qquad \text{Eq. 21.}$$

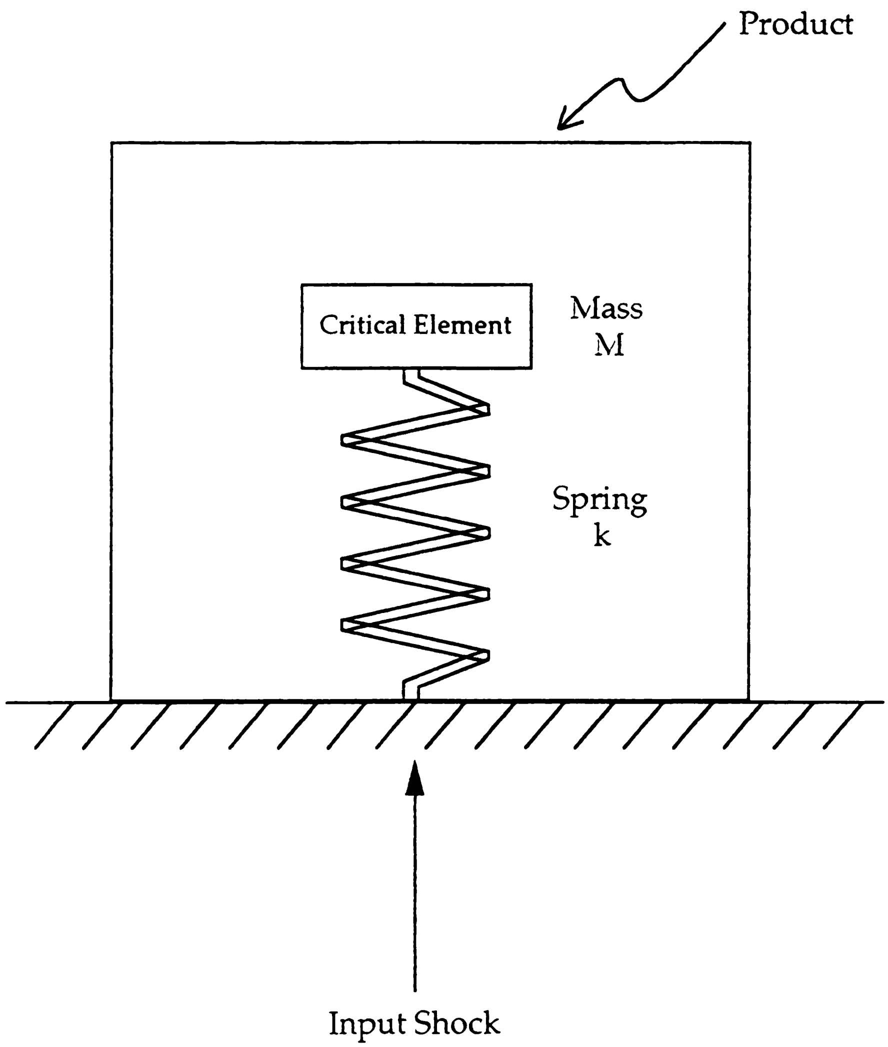

Figure 8. Ideal Model Of A Product With A Critical Element.

where ΔV_{cr} is the critical velocity change required for damage. In other words the product's critical velocity change obtained in the plastic programmer part of the test is related to two properties of the critical element alone: G_{ce} and f_n. In the second part of the test, the gas programmer essentially produces a long duration square wave shock. For the square wave, the response is $G = 2G_{input}$, from Equation 18. Again the critical element fails when the response $G = G_{ce}$, so $G_{ce} = 2G_{input}$,

$$\text{or:} \quad G_{cr} = \frac{1}{2} G_{ce}. \qquad \text{Eq. 22.}$$

This says that the product's critical acceleration is half the fragility of the critical element.

Therefore, based on SRS, the results from damage boundary test relate directly to the natural frequency and G_{ce} of the critical element. Conversely, SRS can provide the needed information to construct a DBC without the need for going through the shock machine test procedure, provided that the natural frequency for the critical element is known beforehand. Equations 21 and 22 give the desired information. One way to obtain the required information about the critical element is to perform the gas programmer part of the test exactly as outlined for the DBC and obtain G_{cr}. Then G_{ce} can be obtained from this through Equation 22. The natural frequency f_n can then be determined through a non-destructive test by vibrating a new product on a vibration table and recording the table frequency at which the critical element resonates: this is f_n. Now the products critical velocity change can be obtained through Equation 21. The utility of this approach is that only one product need be destroyed compared to the conventional DBC test procedure.

The SRS relations in Equations 21 and 22 can also be used to check the validity of the entire model behind the DBC. Eliminating G_{ce} between Equations 21 and 22 gives a prediction for the natural frequency of the critical element based on the results of the DBC test:

$$f_n = \frac{G_{ce} g}{2\pi \Delta V_{cr}}. \qquad \text{Eq. 23.}$$

A quick check of the natural frequency on a vibration table can confirm this relationship.

There is an inherent problem with the damage boundary curve results since damage occurs before the last drop but after the next-to-last drop because of the way the drop tests are carried out. For example, damage may have occurred at a ten inch drop on the plastic programmers, but not at nine inches. So the damage just occurs somewhere between nine and ten inches. In a 10" drop on the plastic programmers, the velocity change may be 150 in/sec, and at 9" it may be 140 in/sec. Likewise, on gas programmers, damage may occur at 200 psi but not at 175 psi, corresponding to 25 and 20 G's respectively. This then means that the natural frequency of the critical element is somewhere between $\frac{20 \times 386.4}{\pi \times 150} = 16Hz$ and $\frac{25 \times 386.4}{\pi \times 140} = 22Hz$. The assumed model of the product is therefore considered to be correct if the resonance test on the vibration table produces a resonant (natural) frequency between 16 and 22 Hz.

To avoid ambiguity, the last drop is often used to determine the critical acceleration and critical velocity change, and it is obvious now that the damage boundary curve becomes a very conservative tool for identifying fragility. There is always the potential for significantly overshooting the true fragility of an element while at the same time not being sure of its exact fragility. So how does one know if the product can be accurately modeled as in Figure 8 and at the same time obtain accurate fragility levels? This can be answered either by making the check described in Equation 23 with more accurate (more refined) values for G_{cr} and ΔV_{cr}, or by applying SRS to the two waveforms that just cause damage in the DBC test. The steps are:

1) Drop the product on the plastic programmers from a height that just causes damage, and then do an SRS plot on that pulse.

2) Drop a new product on gas programmers as described earlier, and do an SRS plot on that pulse.

3) Overlay the plots from 1 and 2. The intersection point identifies the natural frequency and critical G level for the critical element.

4) Get the natural frequency of the critical element on a vibration table. If the frequencies in Steps 3 and 4 do not match, then the system does not behave like an ideal spring/mass system. If the product is modeled accurately, then any two input shocks that just cause damage will intersect at the natural frequency and G_{cr} of the critical element. The implications of this are far reaching, since it means that determining the fragility of a product containing a critical element could be done simply by using a free fall drop tester. The shape of the input shock pulse is not the determining factor: the response to the input is all that matters. The SRS approach requires only the natural frequency of the critical element and any input waveform that just damages it to determine the complete fragility picture.

2.3 SRS AND DAMPING RATIO

One crucial assumption for the aforementioned model is that it does in fact behave as a linear nondamped spring/mass system. However, there are no real ideal undamped systems, so all models should incorporate some degree of damping. Most commercial software packages for SRS allow for damping.

Damping simply means that after a system is set into oscillating motion, the movement will gradually die out.

The degree of damping is usually specified by a "damping ratio", which has a value between 0 and 1. A damping ratio of 0 means the system vibrates indefinitely. A damping ratio of 1 corresponds to a system with no cycle of motion (the mass returns to equilibrium position immediately after being disturbed). A damping ratio in-between corresponds to a system which gradually dies out as shown in Figure 9. It is possible to incorporate damping into the model and evaluate the shock response. This is done in commercial software packages for SRS. The approach is the same as the ideal model, except that a dashpot is included in the damped model. It is usually the case that the peak response of the mass is smaller with damping than without. Using an SRS plot with no damping to assess the effect of an input shock on a spring/mass system therefore overestimates the effect. With damping included in the analysis, there are now two properties of the system which determine the response to a shock: its natural frequency and its damping ratio. For a real system, both can usually be determined by mounting an accelerometer on the mass, disturbing it (by tapping it or dropping it), and analyzing the response. The natural frequency is easily determined by simply counting the number of cycles per second. The damping ratio can be calculated by measuring the decay in the peak heights of the recorded waveform.

The first method used in this study to estimate the damping ratio of a beam was to count the number of cycles, N, the beam oscillated through before returning to rest. The damping ratio then is:

$$\text{Damping Ratio} = \frac{1}{\sqrt{1+N^2}} \qquad \text{Eq. 24.}$$

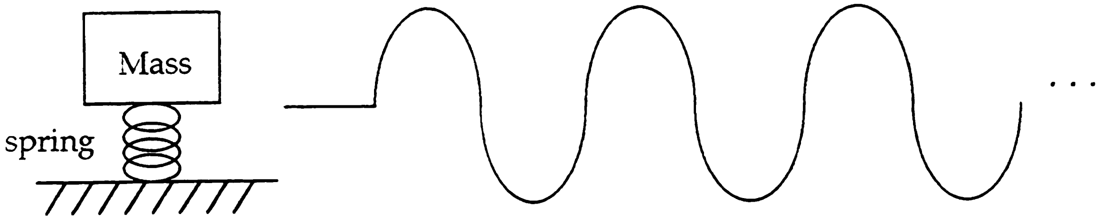

The ideal system vibrates indefitenely

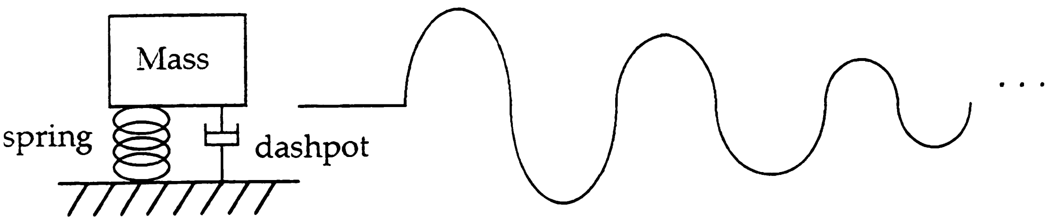

A real system dies out gradually

Figure 9. Damped And Undamped Systems.

where: N = the approximate number of peaks before the system dies out.

The second method uses the successive peak heights of the decaying waveform to determine damping ratio. In Figure 10 the peak heights are labeled H1, H2, etc. This method is described by the equation:

$$\text{Damping Ratio} = \frac{\ln\frac{H_1}{H_2}}{\sqrt{(\ln\frac{H_1}{H_2})^2 + 4\pi^2}} \qquad \text{Eq. 25.}$$

Where: H_1 = acceleration in G's of the first peak

H_2 = acceleration in G's of the second peak

Since the damping ratio is a property of the system, $\frac{H_1}{H_2} = \frac{H_2}{H_3} = \frac{H_3}{H_4} = etc.$

Experimentally determined damping ratios will be used later to check the ability of a commercial software to do SRS plots on systems with damping. The derivations of the above equations can be found in Appendix C.

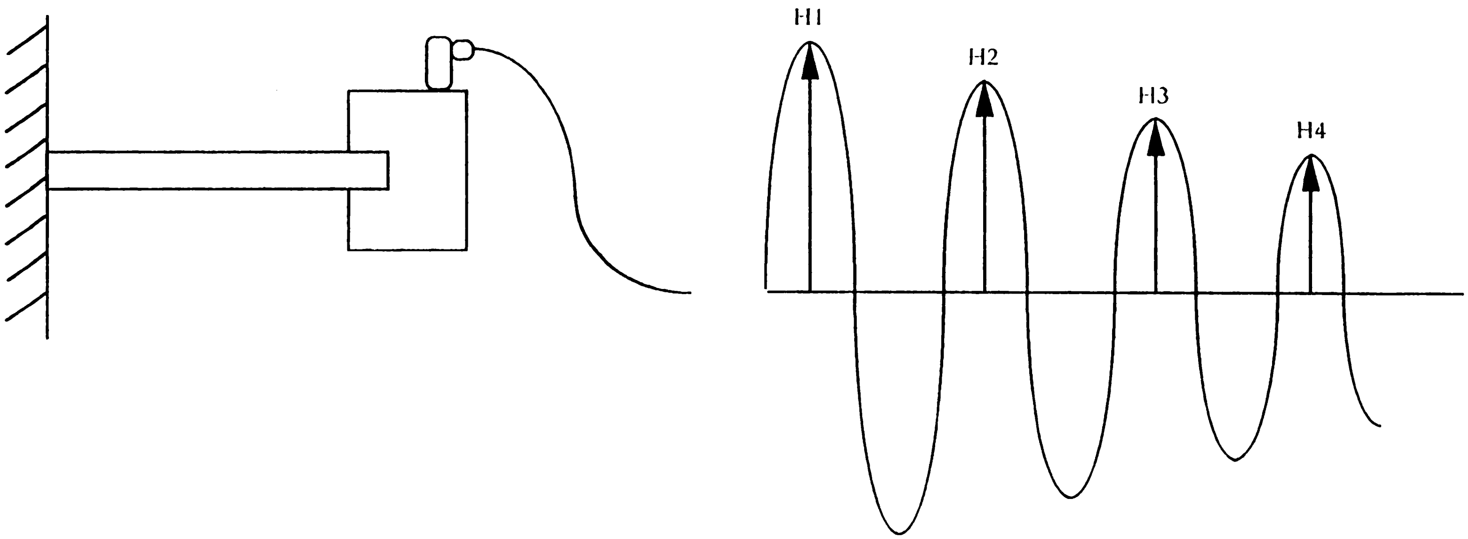

Figure 10. Determining Damping Ratio Using Successive Peak Heights After Setting Beam Into Motion.

CHAPTER 3

MATERIALS AND TEST METHODS

3.1 SOFTWARE

Computer software and hardware from the Lansmont Corporation was used to evaluate the responses to input shocks during testing. Specifically, Test Partner 2 (TP2) was used. Test Partner captures analog acceleration versus time signals from shocks. The data is digitized and processed in a number of different ways. The system features include the following:

- Four channel data capture
- High-resolution color displays
- 1MHz 12 bit analog-to-digital conversion
- Support for dot, color and laser printers
- Support for keyboard, mouse and touchscreen input devices
- Automatic non-destructive digital filtering
- Automatic or manual analysis
- Analysis modes tailored to specific waveforms
- Peak and minimum acceleration, durations
- Velocity change calculation
- Trace shift and zoom
- Triaxial resultant vector magnitude
- Deflection calculation and display
- Extended transient computation
- Mil-spec tolerance bands
- Shock response spectrum (SRS) analysis
- Shock response time domain (SR) analysis

3.2 EQUIPMENT

Accelerometers:	1. Dytran, Model 301UA5, S/N 612
	2. Kistler, Model 818, S/N 2834
Charge Amps:	Kistler Piezotron Coupler, #5112
Cables:	Coaxial Belden 8263 Shielded.
Shock Table:	Lansmont Model 65/81, Serial Number 57-681-0016
Vibration Table:	Lansmont Touchtest Vibration System
	Model 10000-10, Table size 152 cm, Hydraulic Power Supply
Oscilloscope:	Kikusui Electronics Corporation
	CO S5020-ST Storage Oscilloscope 20 MHz
Drop Tester:	Lansmont Model PDT-56E Free Fall Drop Tester

3.3 TEST METHOD FOR SRS EVALUATION

The objective of this test procedure was to evaluate the ability of SRS to accurately predict the response of a product to an input shock. By necessity, this procedure also tests the validity of the model of a product as a linear damped spring/mass system. This was done by evaluating the accuracy of the SRS analysis of two different input pulses, using the known damping ratio and natural frequency of the system. The models used were two different metal beams, each with a mass attached to one end. One beam (referred to as the fixed beam) was tested at only one length, corresponding to a natural frequency of 14.3

Hz. The second beam (referred to as the variable beam) was affixed in varying lengths so as to vary the natural frequency of the system. See Figure 11 (variable beam setup in the 20.2 Hz position). The beams were held in place with clamping plates fastened to a wood mounting.

An accelerometer was mounted on the mass in order to measure the response. For purposes of modeling, the accelerometer was assumed to be a part of the mass, and natural frequencies were determined with the accelerometer attached. The steps involved in the evaluation process were as follows:

Step 1. Determine the damping ratio of the beam. Two methods were used. The beam was set into motion by hand and the decaying output acceleration signal was captured on a storage oscilloscope. The storage scope was equipped with an output channel, so the signal was also fed into TP2. The oscillation was captured by both the oscilloscope and Test Partner simultaneously. Equation 24 determined damping ratio by counting the approximate number of cycles of oscillation before the beam returned to rest from the oscilloscope. Equation 25 was used by taking the peak G's from successive peak heights using TP2. The results using Equation 24 and the oscilloscope are found in Appendix D.

Step 2. Determine natural frequency of the beam. The method used to determine the natural frequency of each spring/mass system was to place the system on a vibration table and perform a sine sweep test as outlined in ASTM D999 [17]. A .5 G input and 3 to 100 Hz sweep was used, to look for resonance. The resonant frequency was then taken to be the natural frequency. At this point, we now know the two properties of the spring/mass system needed to do an SRS plot (f_n and damping ratio).

Step 3. The third step was to determine if the predicted SRS from a particular input shock matched the actual response of the beam. The unit was

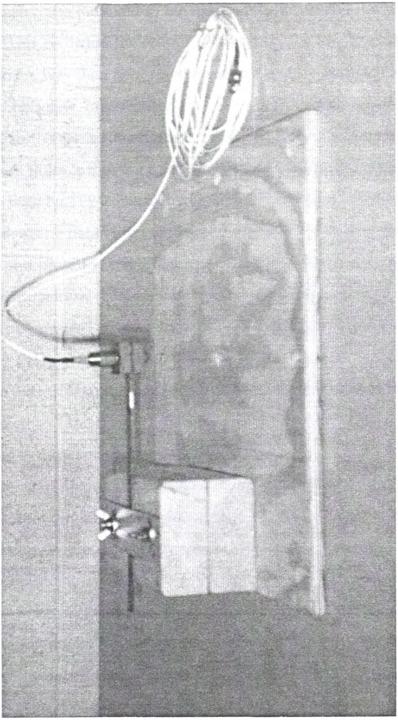

Figure 11. Linear Damped Spring/Mass System With Accelerometer Attached.

mounted on the shock machine. An accelerometer attached on the shock table (to measure the input acceleration) was routed to channel one on TP2. Another accelerometer was mounted to the mass on the beam and routed to channel two on TP2. This recorded the output acceleration. A low level drop onto plastic programmers was then performed, using a height of two inches. Both the short duration half-sine input pulse and the output response of the beam were recorded in the same time domain. Refer to Figure 3. When evaluating each input shock pulse, a filtering frequency of zero was chosen. This unfiltered spike was then used by TP2 to calculate the SRS. Acceleration levels were affected very little by choosing not to filter the input pulse, and no filtering gave the worst case scenario and provided consistency in evaluation. The peak acceleration at each of the beams' natural frequency was then compared to the actual response of the beam. This comparison was done using no damping (damping ratio = 0), and using the calculated damping ratios from experimentation. Using the shock response (SR) time domain function of TP2, the natural frequency of the beam was entered and the theoretical shock response to the beam was calculated and compared to the actual response of the beam.

Step 4. The procedure in Step 3 was duplicated using gas programmers. A table height of eight inches and a pressure of 150 psi was used for each drop. The filtering frequency used for the input shocks was the default frequency, which was usually about 370 Hz. Too much filtering destroyed the integrity of the trapezoid pulse, and there were negligible differences of G levels in the SRS when filtered at 200 Hz, so the shock response was calculated using the pulse filtered at the default frequency. Theoretically, the damping ratio is a property of the spring/mass system, so acceleration levels were compared using the same damping ratios as in Step 3 for each beam.

3.4 TEST METHOD FOR DEFLECTION FAILURE

To test the prediction for deflection failure, (Equation 20), a new beam with a natural frequency of 17 Hz was mounted to the setup in Figure 11. The height from the bottom of the mass to the surface below was measured. The height of the beam above the surface was adjusted to give two different heights from which to test. The first height was 15/16" (.9375"), and the second was 1 3/8" (1.375"). The drops were done using the plastic programmers, and the table height was raised incrementally until the bottom of the mass made contact with the surface below. Contact was evident from looking at the indentation on the wooden surface, and the small spike present in the captured waveform. See Figure 12. TP2 was then used to generate an SRS on the pulse, and the peak G was used with Equation 19 to predict the deflection. This predicted deflection was then compared to the known measured distance. Since damping ratios for the beam were so low (< .1), they were not considered in the calculation, as it would have little effect. See Appendix E for using damping ratio with deflection failure.

3.5 TEST METHOD FOR FRAGILITY TESTING

The objective of this part was to test the widely used assumption that an element of a product fails when its peak acceleration reaches a certain level. In other words, a critical element inside a product fails when the product gets any kind of shock which produces a prescribed G-level to the element. A second objective is to show that a DBC can be constructed from damage information obtained from drops done on equipment other than the shock machine. The wooden box in Figure 13 was used as the model. For this thesis, the product used was a wooden box with no lid containing a plastic rectilinear piece attached to the box on one end, and weighted with a metal mass on the other end.

Deflection Failure
DEF3.PL2

2:04:36 PM
09-03-1993

	Channel 1	Channel 2	
Faired Acc:			G's
Peak Acc:	220.62	72.30	G's
Min Acc:	-13.22	-22.41	G's
Duration:	1.80	14.80	msec
Delta V:	92.68	149.34	In/S
Filter:	500	676	Hz

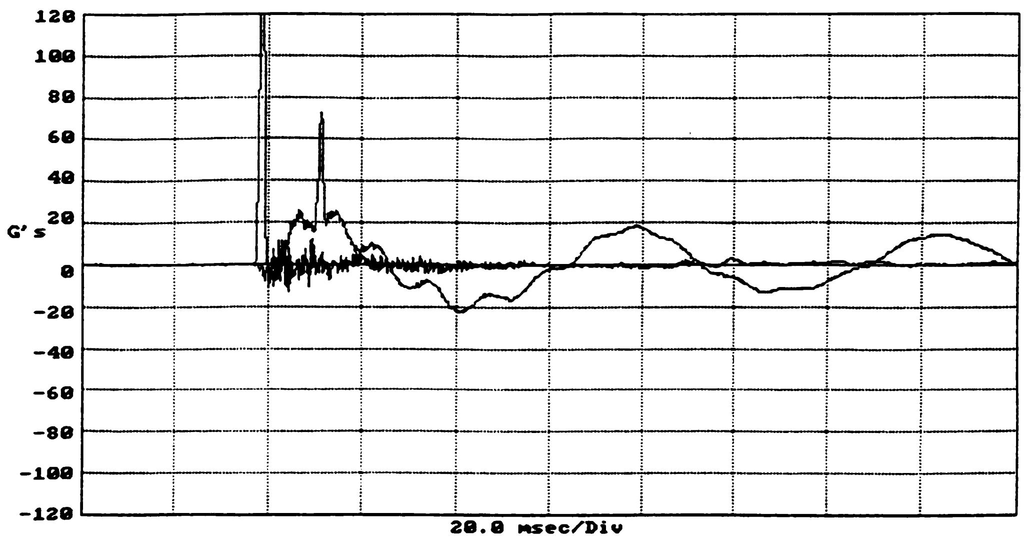

Notes: Deflection failure testing
4 inch drop onto plastic programmers
Plastic Beam with natural frequency of 17 Hz
Maximum allowable deflection: 15/16 inch
Shock response predicts max G of 27.51

Michigan State University

TEST PARTNER

Figure 12. Plastic Programmers Drop Showing Deflection Failure.

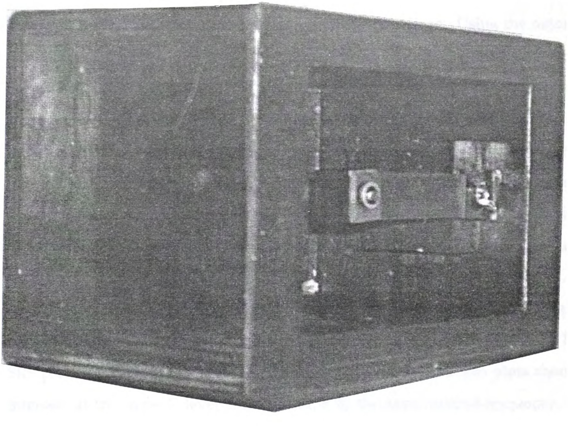

Figure 13. Test Unit Used For DBC.

Damage was defined as the breaking of the plastic beam. Since the beam is the object of interest, we call it the critical element, designating it the most important piece to observe during testing.

Step 1. Find the natural frequency of the critical element. This was done using a vibration table, as in Step 2 of the previous test. The plot of the sine sweep indicated a natural frequency of about 16 Hz.

Step 2. A standard damage boundary test was performed, as outlined in ASTM D3332-77(1983). One accelerometer was mounted on the shock table, and routed to TP2 to capture the pulse of the waveform. The pulses captured were the drop just before failure and the drop that caused failure. Using the natural frequency of the critical element from Step 1 in an SRS plot with no damping, (since damping was quite small), the critical peak acceleration of the plastic beam was predicted. A range of natural frequencies within which the beam should fall into can be found using the above information since damage occurs somewhere between the drop height increments. This is also a good way to test the accuracy of the model as a linear spring/mass system. The critical G is between the two drops, since failure occurs at one and not the other, and it is not known if the last drop height that caused failure is the borderline failure.

Step 3. Continue the damage boundary using gas programmers. Again, do SRS plots on the pulses just before failure and the drop causing failure. This SRS plot was compared to the one generated in Step 2. The two plots should intersect at the same G level corresponding to the same natural frequency. If they are somewhat close, the probable reason is that the spring/mass system is slightly damped. If they are not close, the system is probably not modeled accurately.

Step 4. Perform a free fall drop test onto two different cushions. This step was done to change the shape of the input shock. The two previous steps

generated a square wave input and a half-sine spike. This step produced input shocks of considerable shape difference. A corrugated box was constructed to house the test unit, with space left for the insertion of a cushion. The first cushion used was a high density polyethylene 220 foam. Two planks were cut, each 2 1/8 inches high by 2 1/2 inches wide by 15 inches long. They were placed on opposite edges under the test unit's bottom side. This set-up attempts to simulate a product resting on its cushion in a normal drop test situation. The second foam was low density polyurethane. This material was two inches deep, and covered the entire bottom surface of the test unit. The test procedure began by dropping the unit from 17 inches using a Lansmont free fall drop test machine. If no failure occurred at the drop height, the height was raised by increments of two inches until the plastic beam broke. Each pulse was captured for analysis. This procedure was done for the polyethylene foam and for the polyurethane foam. For each pulse causing damage, an SRS plot was generated and compared to those from Steps 2 and 3. Again, it is expected that they should intersect close to the same G level and natural frequency of the beam. Using the known natural frequency and critical element fragility from the above drops, the same damage boundary curve generated from the traditional method was generated using the information obtained from the intersection points on the SRS plots, and Equations 21 and 22.

CHAPTER 4

RESULTS

4.1 RESULTS

4.1.1 Results From Damping Ratio

Table 1 shows the results using Equation 24 and the decaying waveform read from the oscilloscope. Table 2 shows the results using Equation 25 and the peak heights of the decaying waveform captured by TP2. There is no significant difference between the two methods in terms of the overall damping ratio average for each natural frequency. The damping ratio of .04 for the 50 Hz beam using Equation 24 appears to be a bit high. A probable reason is the stiffness of the beam, which produces very small oscillations making them very difficult to read from the oscilloscope. Also, since the beam's length was shortened to obtain 50 Hz, disturbing the mass produces higher strain than for a longer beam. Thus we would expect the damping ratio to be slightly higher for the higher natural frequency. However, the damping ratio for all four natural frequencies is below .1, which is very low, and hence not significantly different than a damping ratio of 0, as will be shown shortly with the results from SRS. (Figure 14).

4.1.2 Results From Plastic Programmers.

Table 3 shows the results from Step 3 of the first procedure. The values reflect the average of five trials performed at the same conditions for each set-up. The four different natural frequencies were subjected to the same two inch drop onto the plastic programmers, and the actual response was captured. Both the input and output pulses were not filtered for evaluation.

Table 1. Damping Ratio Using Equation 24.

Beam Frequency	9.5 Hz	14.3 Hz	20.2 Hz	50 Hz
Average Damping Ratio	.02	.03	.02	.04

Table 2. Damping Ratio Using Equation 25.

Beam Frequency	9.5 Hz	14.3 Hz	20.2 Hz	50 Hz
Average Damping Ratio	.02	.06	.02	.02

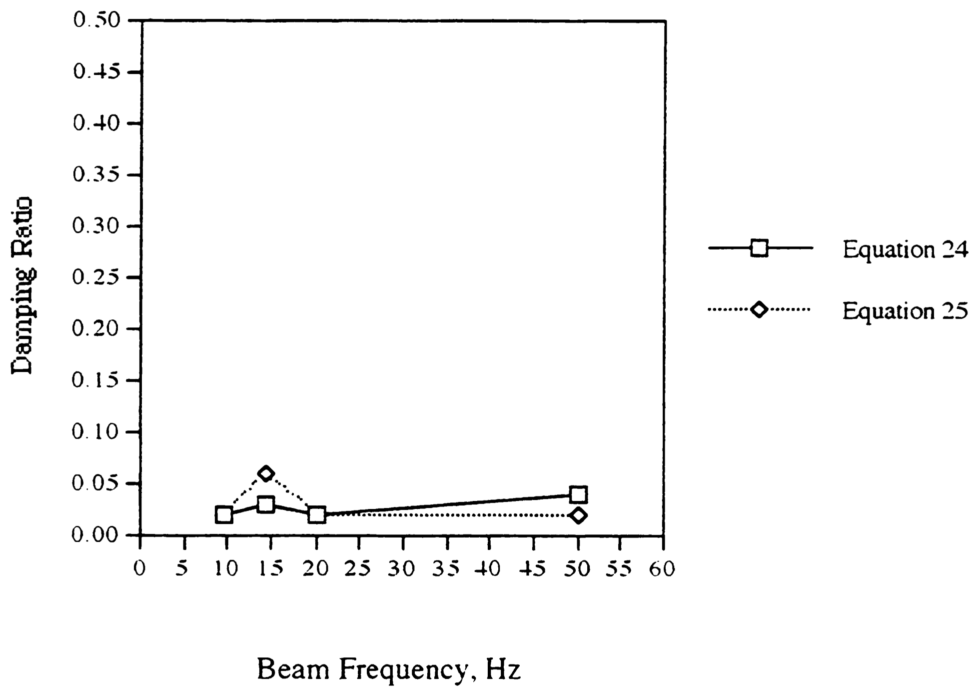

Figure 14. Damping Ratio Comparison Between Equation 24 and Equation 25.

Table 3. SRS Evaluation Results and Comparisons.

PLASTIC PROGRAMMERS

	9.5 Hz	14.3 Hz	20.2 Hz	50 Hz
Actual Output Acceleration, G's	12.35	11.50	19.02	48.08
Damping Ratio	0.00	0.00	0.00	0.00
SRS Peak Acceleration G's	11.10	13.06	20.89	49.63
Damping Ratio	0.00	0.00	0.00	0.00
Peak Acceleration, G's D.R. Eq. 24	9.17	11.34	17.00	43.77
Damping Ratio	0.02	0.03	0.02	0.04
Peak Acceleration, G's D.R. Eq. 25	9.76	11.19	17.00	45.78
Damping Ratio	0.01	0.04	0.02	0.01

GAS PROGRAMMERS

	9.5 Hz	14.3 Hz	20.2 Hz	50 Hz
Actual Output Acceleration, G's	N/A	24.89	21.76	31.24
Damping Ratio		0.00	0.00	0.00
SRS Peak Acceleration G's	N/A	26.06	28.54	29.31
Damping Ratio		0.00	0.00	0.00
Peak Acceleration, G's D.R. Eq. 24	N/A	24.91	27.66	27.50
Damping Ratio		0.03	0.02	0.04
Peak Acceleration, G's D.R. Eq. 25	N/A	24.56	27.66	28.77
Damping Ratio		0.04	0.02	0.01

9.5 Hz Beam. In all five drops, the actual output G's was slightly higher than the theoretical G level predicted by SRS with zero damping. The damping ratios calculated by Equations 24 and 25 were also used to calculate SRS by TP2, as Table 3 shows. A damping ratio of 0 gives the most accurate results, but even with a damping ratio of .02 the actual and predicted G's differed by less than three and one-half G's. In this case, for such a low natural frequency, 0 damping is most accurate. To verify the prediction of TP2 of the shock response to a spike, we can check it against Equation 7. The natural frequency is known, and the value used for ΔV was calculated by TP2 (done digitally by integration). The input pulse is a short duration spike (from the pulse BRESK, the third trial), and has a peak G of 121 and a duration of 2.4 ms. So from Equation 7: peak G = $2\pi f_n \Delta V / g = 8.80$ when using the ΔV from TP2. The actual G level was 11.87 , and SRS predicted 10.75 G, with no damping.

14.3 Hz Beam. SRS predicted results very similar for all damping ratios compared to the actual G level. In most cases the G's differ only by one or two. The check on pulse YRES1, the first trial, using Equation 7 reveals: Peak G = 13.77 when using the ΔV from TP2 analysis. These values compare with the actual of 11.53 G and the SRS value calculated as 13.60 G, with no damping.

20.2 Hz Beam. The damping ratio calculated for this frequency was about .02. For plastic programmers, no damping produced higher G's than the actual and damping of .02 produced slightly lower G's suggesting there is some damping. It should be stressed this small level of damping is negligible. Using Equation 7 on pulse BRES4, the second trial: Peak G = 18.62 using ΔV from TP2. The actual response was 19.04, and TP2 calculated a peak G of 20.59 with no damping. There are very small differences between these calculations, suggesting TP2 and Equation 7 give accurate results.

50 Hz Beam. Using no damping TP2 predicted G's slightly higher than the actual, and damping ratios of .01 and .04 predicted G's slightly lower. Again, there are very small differences, and using no damping gives very accurate results. From Equation 7 and ΔV from TP2: Peak G = 48.58 for pulse BRESE, trial five. Compare that to the actual of 49.80 G's, and TP2 calculating 49.95 G's using SRS.

4.1.3 Results From Gas Programmers.

For the gas programmers, the beams with different natural frequencies were subjected to the same eight inch drop height, 150 psi square wave shock, and the response was recorded. The results are also shown in Table 3. Again, the values reflect an average from five trials for each set-up.

9.5 Hz Beam. Only one drop was completed, since the shock was too severe for this setup. The beam bent, so testing was stopped. However, based on the input square wave, the predicted G from TP2 was 22.46 G's. Since T < $\frac{1}{2f_n}$, we would expect the peak response of the beam to be $G_{in}\sqrt{2(1-\cos\omega T)}$ and the peak occurring sometime after the duration of the square wave. The input acceleration reaches a peak of 14.89, and the duration of the pulse is about 27 ms. The predicted G is therefore 22.32 G's. This is essentially the same as calculated by TP2.

14.3 Hz Beam. The actual G's and G's predicted by TP2 with 0, .03, and .06 damping ratio were all very similar. TP2 predicts a peak G response of 26.02 G's, and from Equation 19, G is predicted to be 28.06. The small discrepancy can be attributed to the peak acceleration of the input shock (14.98), which is not really constant over the pulse's duration.

20.2 Hz Beam. For this case, T is about equal to $\frac{1}{2f_n}$ so the peak G response should occur almost exactly at the end of the input shock (where t = T). Since $T \geq \frac{1}{2f_n}$, the SRS G's should be twice the input shock acceleration. This set-up produced the largest discrepancy between the actual and predicted G level. The actual output averaged 21.76 G's and SRS predicted an average G of 28.54. Although the G level is different, the predicted is still slightly larger, so a worst case scenario situation is produced. A possible explanation for the difference could be that the beam is not really 20.2 Hz. More likely, the duration of the pulse is very near the breakpoint between Equation 17 and Equation 18, so TP2 may have chosen to treat the square wave as being long enough to double its acceleration level.

50 Hz Beam. Here, $T > \frac{1}{2f_n}$, so the peak response G will occur sometime during the duration of the input pulse. This is in fact what does occur. The peak G using the peak from the input shock BRESF and Equation 19 should be 29.78 G, and TP2 predicts 29.01. Again, the small difference can be attributed to the fact that the acceleration of the "square wave" produced by the gas programmer is not perfectly constant over its entire duration. The small damping ratios do not differ significantly from a damping ratio of 0. The expected peak G reached during the duration T should be almost exactly $2G_{in}$, since there is very little deflection of the beam. Less deflection of the beam will mean the path the beam travels in during motion will be more linear, not angular, and will more closely model a true spring/mass system.

4.1.4 Results From Deflection Failure.

Using the peak G predicted by SRS from the pulses obtained just at the critical deflection yielded very accurate results. For the 15/16" setup, peak G was 27.52 G's. Using Equation 20, the predicted deflection is then .9320 inches. Similarly, for the 1 3/8" setup, peak G was 40.91 G's, so the predicted deflection becomes 1.385 inches. Obviously SRS is an accurate tool to predict when deflection failure will occur.

4.1.5 Results From Fragility Testing.

A new plastic beam was used for this testing. The natural frequency was determined by finding the resonance on a vibration table. A very small accelerometer with negligible mass was mounted on the weight attached to the end of the beam. The approximate natural frequency was 16 Hz.

To show the system behaves as a linear spring/mass system we can use the results from the damage boundary testing. Performing a damage boundary test revealed that on plastic programmer drops there was no damage at a ΔV of 165.03 in/s, but there was damage at 171.56 in/s. Similarly, for gas programmers, there was no damage at 20.56 G but damage at 23.76 G's. Since we are dealing with a range, the natural frequency can be found within the upper and lower limits of the above results.

$f_n = \dfrac{G_{ce}g}{2\pi\Delta V_{cr}} = \dfrac{20.56 \times 386.4}{\pi \times 171.56} = 14.7\,Hz$ at least, and $\dfrac{23.76 \times 386.4}{\pi \times 165.03} = 17.7\,Hz$ at most. The known natural frequency of 16 Hz falls within this range.

The drops onto the plastic programmers, gas programmers and cushion that broke the beam were all used to construct their respective SRS plots. If SRS is valid in predicting the critical G for an element despite the shape of the input pulse which caused damage, the plots should all intersect at the same natural frequency and critical G level. Overlaying the plots from testing reveals that this is in fact what happens. See Figures 15, 16, 17 and 18. All four plots are composite plots, meaning the minimum and maximum G levels of both the primary and residual responses were plotted. The upper most curve is the maximum response, and the one of interest. All four SRS plots intersect at approximately 16 Hz and roughly 46 G's. The implication is that by using SRS one may obtain the same information for DBC by simply dropping a product from a normal free fall drop tester. This is shown by comparing the SRS data to the damage boundary test results.

From the damage boundary test, ΔV_{cr} was found to be 171.56 in/sec, and G_{cr} was 23.76 G's. These are results taken from the drop that caused damage, so they are conservative and probably represent a slight over-estimation. For consistency, the drops causing damage from the other inputs were also used. From the 21 inch free fall drop onto the polyethylene cushion, (pulse DTB), the SRS plot shows a peak G of 43 G's at 16 Hz. So, using Equations 21 and 22, the same DBC curve can be constructed, since from the SRS plot:

$$\Delta V_{cr} = \frac{43 \cdot 386.4}{2 \cdot \pi \cdot 16} = 165.27 \text{ in/s}$$

$$G_{cr} = \frac{1}{2} G_{ce} \qquad = 21.5 \text{ G's}$$

A check with the SRS plot from a drop onto the polyurethane cushion (pulse K2) yields the same results.

Evaluation of SRS Software
C:\TP2\DATA\DB4.PL2
Channel 1
SRS Type: Composite
Resolution: 20 PPO
Damping: 0.00
Peak Acc: 59.10 G's
Peak Fn: 109.28 Hz
Min Acc: -65.43 G's
Min Fn: 144.20 Hz

12:43:28 PM
05-25-1993

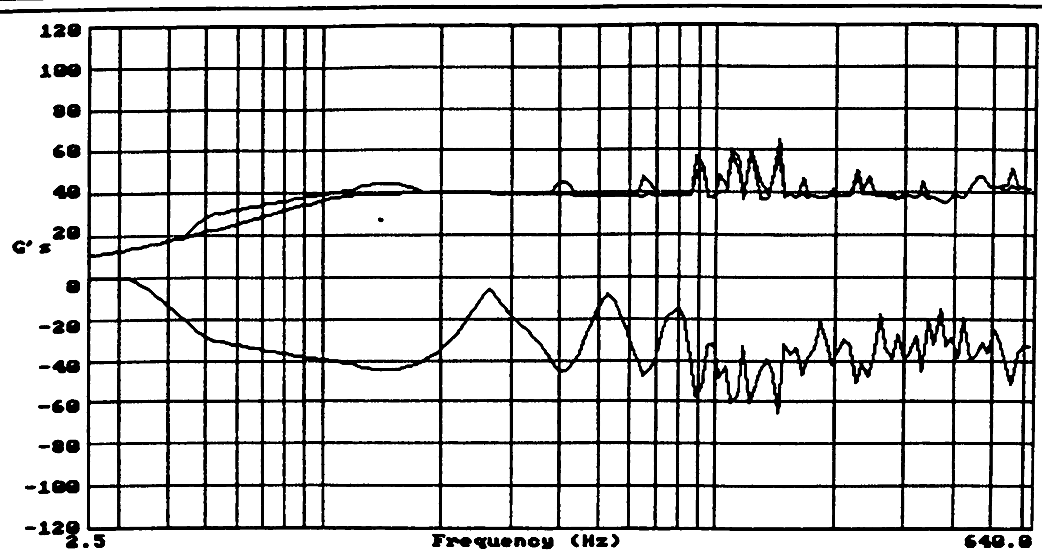

Notes: Plastic Beam, 16 Hz
200 psi
Table Height of 30"
Beam breaks on this drop

Michigan State University

TEST PARTNER

Figure 15. SRS Plot From 30" Gas Programmer Drop.

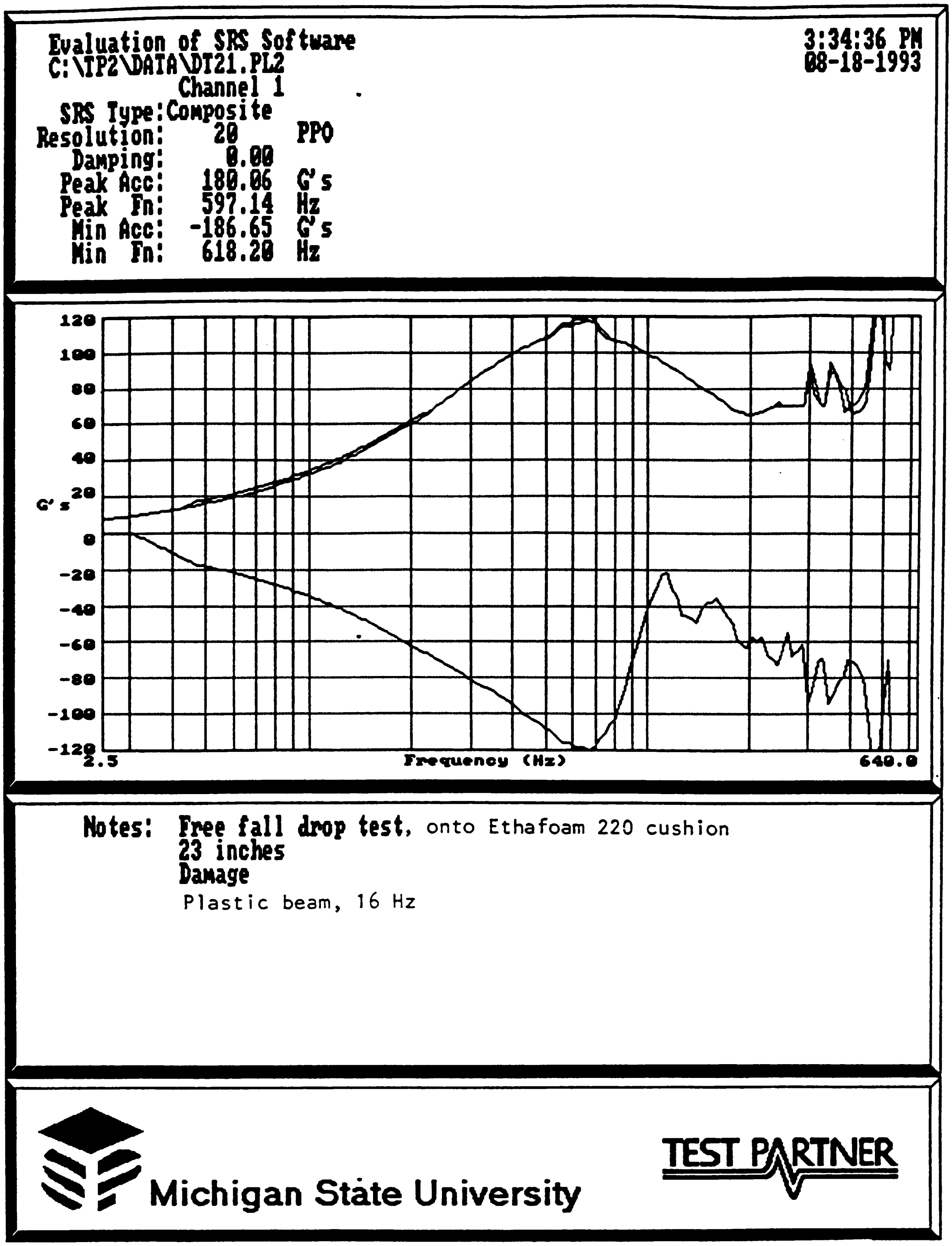

Figure 16. SRS Plot From 23" Free Fall Drop Test Onto Ethafoam 220.

SRS and Damage Boundary
C:\TP2\DATA\DB2.PL2
Channel 1
SRS Type: Composite
Resolution: 20 PPO
Damping: 0.00
Peak Acc: 803.11 G's
Peak Fn: 367.58 Hz
Min Acc: -804.76 G's
Min Fn: 380.55 Hz

12:08:09 PM
05-25-1993

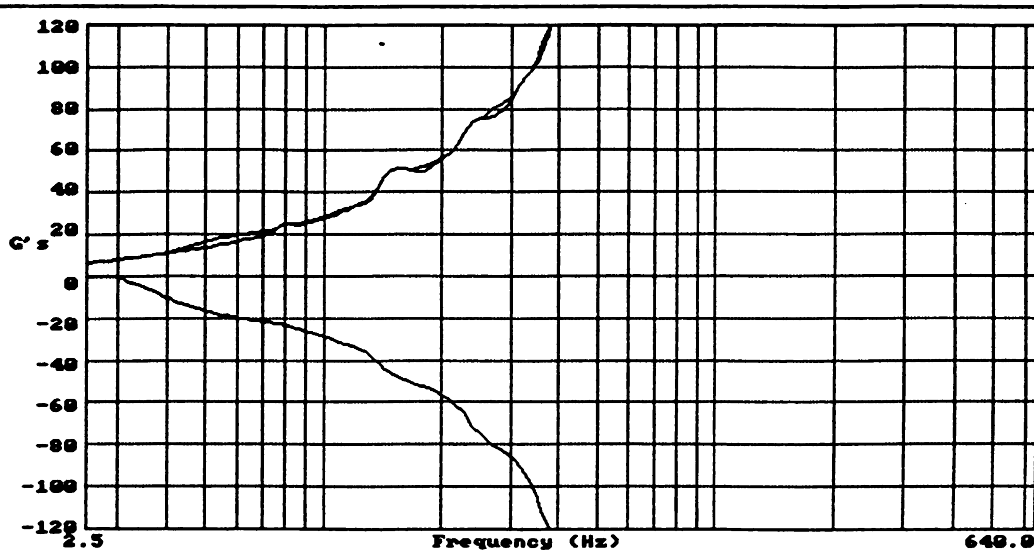

Notes: Plastic Beam, 16 Hz
Plastic Programmers, 17" drop height
Beam breaks on this pulse

Michigan State University

TEST PARTNER

Figure 17. SRS Plot From 17" Plastic Programmers Drop.

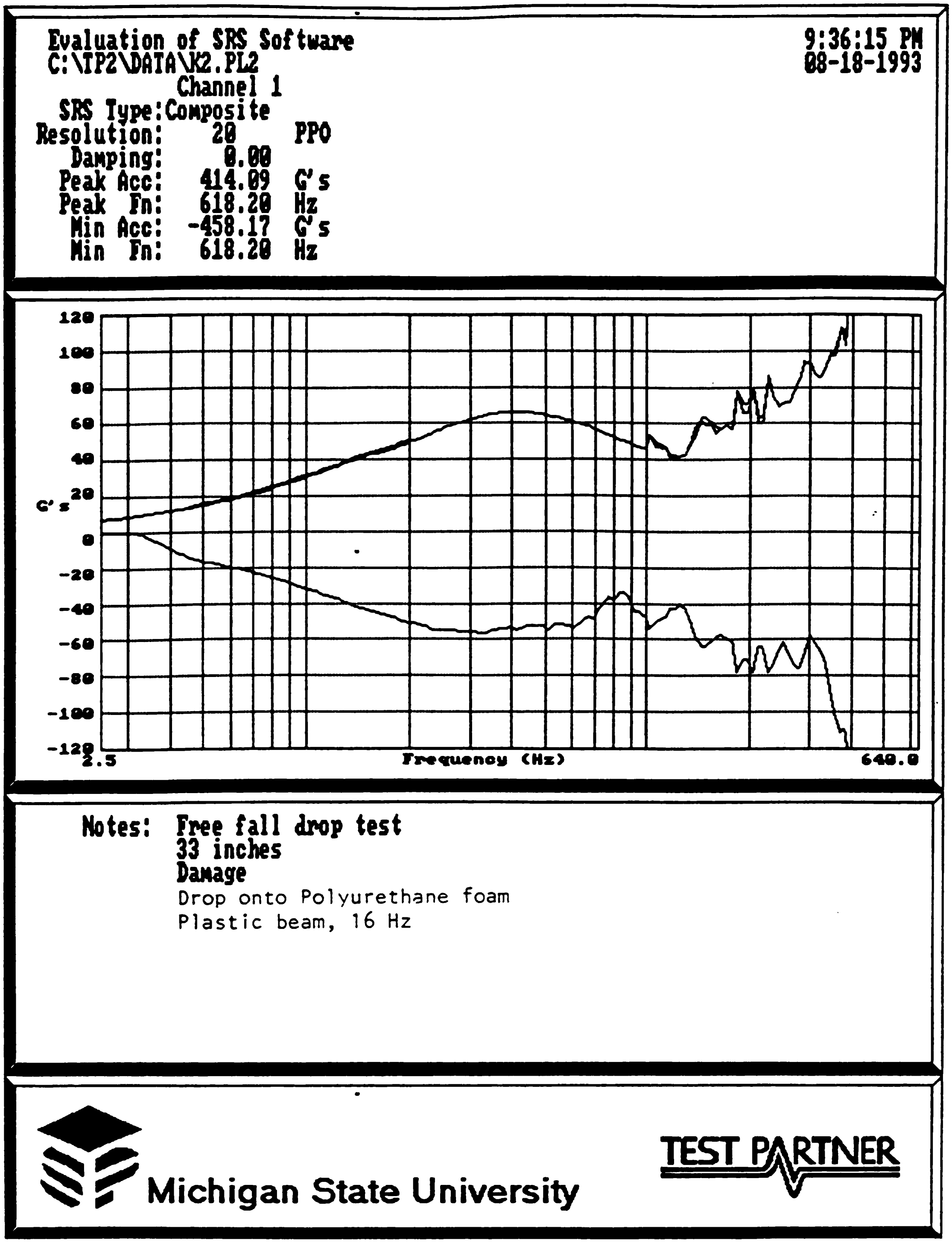

Figure 18. SRS Plot From 33" Free Fall Drop Test Onto Polyurethane Foam.

CHAPTER 5

CONCLUSIONS AND LIMITATIONS

5.1 CONCLUSIONS

TestPartner and Equation 7 accurately predict the actual peak acceleration level with no damping. This suggests the model does in fact behave as a linear spring/mass system. Also, it appears that for very low damping ratios there is not a significant difference from zero damping. Using a damping ratio of 0 for short duration, high acceleration impacts gives very accurate results compared to the actual output. The proposed model for a spring/mass system is accurate, and Equations 18, 19, and TP2 are in agreement with the actual output G levels. SRS can be used confidently to predict the response of a spring/mass system to an input shock.

The results in Figures 15-18 show the predicted response of the critical element was the same for the different input shocks at the time of failure. This result supports the assumption the component fails at a prescribed G level regardless of the source of the shock. This means the same information contained on a damage boundary curve can be extracted easily from any SRS plot that just damages the critical element. The shape of the input pulse does not matter, eliminating the need for a shock table. Thus, the lengthy and costly investment of a DBC testing procedure is reduced to damaging one unit in an inexpensive free fall drop test.

5.2 LIMITATIONS OF SRS

SRS is designed to predict the response of a spring/mass system to a shock, and should therefore not be expected to predict failure in cases where damage occurs to a component that does not behave as such. Products that have no identifiable critical element, specifically the "spring" component, such as glass, or boxes of agricultural products are some examples.

SRS is also limited to products that fail due to some critical G-level, not a critical velocity change. A general rule of thumb is that SRS applies to brittle or stiff products, like the plastic beam that was modeled, or a magnetic head in a VCR. Components that are soft, or ductile, and fail because of velocity change or fatigue will not be treated satisfactorily with SRS.

5.3 FUTURE WORK

Though current commercial SRS software packages accurately calculate SRS plots, there are some useful additions that could be made. In addition to predicting the peak G response of a spring/mass system, the velocity change could also be given, since the required information is already provided. The software could also be improved to allow the user to enter hypothetical shocks. There are instances where the input shock may be known beforehand, so the response could be calculated without the effort of instrumenting a product and performing drop tests. This would eliminate the need for dependence on analog signal hardware.

APPENDIX A

APPENDIX A

To show the peak residual response to a square wave input is $G_{in}\sqrt{2(1-\cos\omega T)}$ for either $T < \dfrac{1}{2f_n}$ or $T \geq \dfrac{1}{2f_n}$, recall Equations 16 and 17.

From Equation 17, when $t > T$,

$$G_{response} = G_{in}\left[\cos\omega(t-T) - \cos\omega t\right] \qquad \text{Eq. 17.}$$

Expand by using the cosine difference identity, and simplify to obtain:

$$G_{res} = G_{in}\left[a\sin\omega t + b\cos\omega t\right] \qquad \text{Eq. 26.}$$

where $a = \sin\omega T$

and $b = (\cos\omega T - 1)$

The amplitude of $a\sin\omega t + b\cos\omega t$ is:

$$\sqrt{a^2 + b^2} \qquad \text{Eq. 27.}$$

So the peak residual response is:

$$G_{res} = G_{in}\sqrt{(\sin\omega T)^2 + (\cos\omega T - 1)^2} \qquad \text{Eq. 28.}$$

or:

$$G_{in}\sqrt{2(1-\cos\omega T)} \qquad \text{Eq. 29.}$$

This is the peak residual response to a square wave input when $t > T$. It is also the peak residual response when $t < T$, since

$$G_{in}(1-\cos\omega T) < G_{in}\sqrt{2(1-\cos\omega T)} < 2G_{in} \qquad \text{Eq. 30.}$$

This is shown by first eliminating G_{in} from each expression. To show that

$$1-\cos\omega T < \sqrt{2(1-\cos\omega T)}, \qquad \text{Eq. 31.}$$

square both sides and simplify to obtain:

$$1+\cos^2\omega T < 2 \qquad \text{Eq. 32.}$$

And this inequality is true because cos ≤ 1.

APPENDIX B

APPENDIX B

The SRS plot for a square wave will start out as a straight line with the same relationship as that of the spike. See Equation 7. To show this, recall the peak primary response when $T < \frac{1}{2f_n}$:

$$G_{in}\sqrt{2(1-\cos\omega T)} \qquad \text{Eq. 29.}$$

For a small natural frequency, estimate the expression $\cos\omega T$ with a power series:

$$\cos\omega T \approx 1-\left(\frac{\omega^2T^2}{2!}\right)+\left(\frac{\omega^4T^4}{4!}\right)\ldots\ldots \qquad \text{Eq. 33.}$$

so:

$$G_{res} \approx G_{in}\sqrt{2\left(1-\left\{1-\frac{\omega^2T^2}{2!}+\frac{\omega^4T^4}{4!}+\ldots\right\}\right)} \qquad \text{Eq. 34.}$$

Since $\frac{\omega^2T^2}{12}$ is small compared to 1 by assumption (i.e. ω T is small), simplify to obtain:

$$G_{in}\omega T \qquad \text{Eq. 35.}$$

Therefore:

$$G_{peak} = (2\pi G_{in}T)f_n \qquad \text{Eq. 36.}$$

Since $(G_{in}g)T = \Delta V$ for a square wave, divide by g and simplify to obtain:

$$G_{peak} = \frac{2\pi f_n \Delta V}{g} \qquad \text{Eq. 37.}$$

which is equal to Equation 7.

APPENDIX C

APPENDIX C

The following is the derivation for each of the damping ratios used in this thesis. Begin with the differential equation of Newton's law of motion, with c representing the dashpot, or damping constant:

$$m\ddot{x} + c\dot{x} + kx = 0 \qquad \text{Eq. 38.}$$

The solution yields:

$$x = A\exp\left(\frac{-c}{2m}t\right)\cdot\left[\cos\omega t + \frac{c}{2mw}\sin\omega t\right] \qquad \text{Eq. 39.}$$

where: m = mass = W / g

c = dashpot constant

k = spring constant

A = amplitude released from

$\omega = 2\pi f_n = \sqrt{\frac{k}{m}}\cdot\sqrt{1-R^2}$

and where R = damping ratio = $\sqrt{\frac{c^2}{4mk}}$.

If you knew m, k and c, then you would know R. But they are never really known, especially c, so R must be obtained by looking at the response of the beam after it is set into motion.

Since the model is an accelerometer mounted on the mass, the output is $\ddot{x}$ versus t (acceleration versus time), not x versus t (position versus time), so take two derivatives of Equation 39, divide by g, and obtain:

$$\frac{\ddot{x}}{g} = G = \frac{kA}{W}\exp\left(\frac{-c}{2m}t\right)\cdot\left(\frac{R}{\sqrt{1-R^2}}\sin\omega t - \cos\omega t\right) \qquad \text{Eq. 40.}$$

All of the above damping ratio equations are based on looking at successive periods of the oscillation:

$$\omega t = 2N\pi \qquad \text{Eq. 41.}$$

where: N = 1, 2, 3, ...

The value of G after the Nth cycle (i.e. the G at the Nth peak) is:

$$G_N = \frac{-kA}{W}\exp\left(\frac{-N\pi c}{mw}\right) \qquad \text{Eq. 42.}$$

Using the starting value of G at time 0 as -kA/w = G_0, substituting variables and rearranging gives:

$$G_N = G_0 \exp\left(\frac{-2N\pi R}{\sqrt{1-R^2}}\right) \qquad \text{Eq. 43.}$$

Solving for R yields the damping ratio:

$$R = \frac{1}{\sqrt{1+Q^2}} \qquad \text{Eq. 44.}$$

where: $Q = \dfrac{2\pi N}{\ln\left(\dfrac{G_0}{G_N}\right)}$.

Equation 44 is the basis for Equation 24. Recall Equation 24 substitutes N for Q, where N is the number of cycles before the system dies out. Making the substitution with N in place of Q uses an arbitrary argument that says the motion of the system *appears* to die out when G_N reaches about .2% of G_0. The .2% is purely arbitrary also, but it is used a lot for many other kinds of exponentially decaying phenomena. So if the motion of the system dies out when $G_0/G_N = 1/.002$, then:

$$Q = \frac{2\pi N}{\ln \frac{1}{.002}} = N \qquad \text{Eq. 45.}$$

So:

$$R \approx \frac{1}{\sqrt{1+N^2}} \qquad \text{Eq. 24.}$$

where: R is the approximate damping ratio

N is the number of cycles before the system dies out.

The second method of determining damping ratio, Equation 25, follows from Equation 43. Equation 25 uses the ratio of two successive peak heights. If the first peak height is noted as G_N, and the next peak height as G_{N+1}, then:

$$G_{N+1} = G_0 \exp\left(\frac{-2(N+1)\pi R}{\sqrt{1-R^2}}\right) \qquad \text{Eq. 46.}$$

or:

$$G_0 \exp\left(\frac{-2N\pi R}{\sqrt{1-R^2}}\right) \exp\left(\frac{-2\pi R}{\sqrt{1-R^2}}\right) \qquad \text{Eq. 47.}$$

Therefore:

$$\frac{G_{N+1}}{G_N} = \exp\left(\frac{-2\pi R}{1-R^2}\right) \qquad \text{Eq. 48.}$$

Solving for R gives:

$$\frac{\ln\frac{H_1}{H_2}}{\sqrt{\left(\ln\frac{H_1}{H_2}\right)^2 + 4\pi^2}} \qquad \text{Eq. 49.}$$

where: H_1 is the peak height, in G's, of the first height

H_2 is the peak height, in G's, of the second height.

APPENDIX D

APPENDIX D

The following is the data collected during the determination of the damping ratio.

In both Table 4 and Table 5, H1, H2, etc., indicate the peak height of the first and second peaks, respectively, after the beam was put into motion. Table 4 reports the peak heights in G's, and Table 5 uses the number of grid divisions read from the oscilloscope. DR followed by two successive numbers indicates the damping ratio between those two peaks. The average under each column is the average damping ratio between all the peaks, and Table 2 reports the average of these five averages. Table 7 is similar to Table 5, except that it applies only to the plastic beam.

Table 6 reports the damping ratio calculated using Equation 24, so N is the number of peaks (cycles) the system oscillated before appearing to die out. The procedure was repeated five times for each natural frequency, so the average from the five trials is reported in Table 1.

Table 8 shows the effect damping ratio has on the prediction of the shock response for each pulse. Each set-up was performed five times for each natural frequency, except for the gas programmers at 9.5 Hz. The column named "Equation 24 Peak G, SRS" reports the peak G's calculated by SRS on TP2 using the damping ratio calculated by Equation 24 for that particular natural frequency. The calculated damping ratio is found in the same column. The column named "Equation 25, TP2 Peak G's" reports the peak G's calculated by SRS on TP2 using the damping ratio that Equation 25 calculated. Similarly, the next column, (with "O" replacing "TP2"), is the peak G's calculated by SRS using the damping ratio obtained from the readings from the oscilloscope and Equation 25. The last column is SRS G's calculated using zero damping. PP represents the results from the plastic programmer drops, and GP represents the results from the gas programmer drops.

Table 4. Damping Ratio Calculations Using Equation 25; Peak Heights Read From Test Partner.

	Variable Beam 9.5 Hz					
	Setting: 10 mv/div .1 sec/div					
	Divisions	**Divisions**	**Divisions**	**Divisions**	**Divisions**	
H1	20.22	22.91	18.76	21.97	21.99	
H2	18.39	19.57	16.78	18.55	19.06	
H3	15.93	17.15	14.35	16.08	16.19	
H4	14.95	16.16	12.97	14.16	15.14	
DR 1-2	0.015097	0.025071	0.017749	0.026921	0.022753	
DR 2-3	0.022849	0.021004	0.024890	0.022736	0.025965	
DR 3-4	0.010105	0.009463	0.016090	0.020233	0.010671	
						Average
Average:	**0.016017**	**0.018513**	**0.019577**	**0.023297**	**0.019796**	**0.019440**
Std. Dev:	0.005243	0.006611	0.003818	0.002759	0.006584	

	Fixed Beam, 14.3 Hz					
	Setting: 10 mv/div .1 sec/div					
	Divisions	**Divisions**	**Divisions**	**Divisions**	**Divisions**	
H1	26.26	35.38	20.92	21.35	21.72	
H2	17.97	23.83	14.08	14.22	14.78	
H3	12.00	17.50	9.31	9.31	9.63	
H4	8.58	12.96	6.30	6.00	6.09	
H5	5.58	9.68	3.83	3.74	3.29	
DR 1-2	0.060265	0.062774	0.062893	0.064546	0.061153	
DR 2-3	0.064134	0.049079	0.065695	0.067259	0.068023	
DR 3-4	0.053316	0.047745	0.062037	0.069751	0.072737	
DR 4-5	0.068316	0.046392	0.078962	0.075016	0.097534	
						Average
Average:	**0.061508**	**0.051498**	**0.067396**	**0.069143**	**0.074862**	**0.064881**
Std. Dev:	0.005520	0.006579	0.006813	0.003858	0.013723	

	Variable Beam, 20.2 Hz					
	Settings: 10 mv/div and .1 sec/div					
	Divisions	**Divisions**	**Divisions**	**Divisions**	**Divisions**	
H1	20.13	13.97	13.87	20.77	17.37	
H2	17.43	12.02	11.76	17.34	14.46	
H3	14.99	10.69	9.99	13.93	12.35	
H4	13.02	9.23	9.03	11.95	10.58	
H5	11.38	8.24	8.05	10.00	9.55	
H6	9.62	7.14	7.07	9.05	8.58	
H7	8.52	6.29	6.46	8.07	7.65	
DR 1-2	0.022915	0.023921	0.026255	0.028715	0.029170	
DR 2-3	0.023995	0.018660	0.025953	0.034829	0.025096	
DR 3-4	0.022419	0.023365	0.016078	0.024393	0.024612	
DR 4-5	0.021422	0.018055	0.018281	0.028341	0.016299	
DR 5-6	0.026731	0.022799	0.020656	0.015885	0.017044	
DR 6-7	0.019322	0.020169	0.014359	0.018238	0.018257	
						Average
Average:	**0.022801**	**0.021161**	**0.020264**	**0.025067**	**0.021746**	**0.022208**
Std. Dev:	0.002274	0.002311	0.004559	0.006464	0.004805	

	Variable Beam, 50 Hz					
	Settings: 10 mv/div and .1 sec/div					
	Divisions	**Divisions**	**Divisions**	**Divisions**	**Divisions**	
H1	21.88	27.29	20.89	33.94	25.94	
H2	18.95	24.85	18.94	30.52	24.12	
H3	16.99	20.95	17.42	25.63	20.49	
H4	15.04	18.51	14.82	20.75	17.30	
H5	13.09	16.55	12.61	19.78	15.35	
DR 1-2	0.022876	0.014905	0.015594	0.016902	0.011577	
DR 2-3	0.017374	0.027161	0.013313	0.027781	0.025950	
DR 3-4	0.019399	0.019704	0.025718	0.033597	0.026924	
DR 4-5	0.022096	0.017811	0.025693	0.007619	0.019030	
						Average
Average:	**0.020436**	**0.019895**	**0.020080**	**0.021475**	**0.020870**	**0.020551**
Std. Dev:	0.002189	0.004530	0.005683	0.009995	0.006169	

Table 5. Damping Ratio Calculations Using Equation 25; Peak Heights Read From Oscilloscope.

	Variable Beam, 9.5 Hz					
	Setting: 10 mv/div .1 sec/div					
	Divisions	**Divisions**	**Divisions**	**Divisions**	**Divisions**	
H1	2.00	2.50	2.10	2.40	2.70	
H2	1.70	2.00	1.60	1.80	2.00	
H3	1.50	1.70	1.40	1.60	1.80	
H4	1.30	1.50	1.20	1.40	1.50	
H5	1.10	1.30	1.00	1.20	1.30	
DR 1-2	0.025857	0.035492	0.043239	0.045738	0.047709	
DR 2-3	0.019916	0.025857	0.021247	0.018742	0.016766	
DR 3-4	0.022769	0.019916	0.024526	0.021247	0.029005	
DR 4-5	0.026578	0.022769	0.029005	0.024526	0.022769	
						Average
Average:	**0.023780**	**0.026009**	**0.029505**	**0.027564**	**0.029062**	**0.027184**
Std. Dev:	0.002650	0.005864	0.008394	0.010692	0.011603	

	Fixed Beam, 14.3 Hz Kistler Acc S/N 612					
	Setting: 10 mv/div .1 sec/div					
	Divisions	**Divisions**	**Divisions**	**Divisions**	**Divisions**	
H1	3.00	3.90	2.20	2.40	2.50	
H2	2.40	3.20	1.90	1.90	2.00	
H3	1.60	2.10	1.20	1.20	1.30	
H4	1.00	1.50	0.80	0.80	0.80	
H5	0.70	1.10	0.50	0.50	0.30	
H6	0.50	0.80	0.30	0.30	0.20	
H7	0.30	0.50	0.10	0.10	0.10	
DR 1-2	0.035492	0.031469	0.023326	0.037155	0.035492	
DR 2-3	0.064398	0.066888	0.072942	0.072942	0.068401	
DR 3-4	0.074595	0.053475	0.064398	0.064398	0.077041	
DR 4-5	0.056675	0.049303	0.074595	0.074595	0.154236	
DR 5-6	0.053475	0.050619	0.081033	0.081033	0.064398	
DR 6-7	0.081033	0.074595	0.172237	0.172237	0.109653	
						Average
Average:	**0.060945**	**0.054391**	**0.081422**	**0.083727**	**0.084870**	**0.073071**
Std. Dev:	0.014853	0.013728	0.044779	0.041999	0.037894	

	Variable Beam, 20.2 Hz					
	Settings: 10 mv/div and .1 sec/div					
	Divisions	**Divisions**	**Divisions**	**Divisions**	**Divisions**	
H1	2.10	1.30	1.50	2.40	1.90	
H2	1.90	1.30	1.30	2.00	1.60	
H3	1.60	1.10	1.10	1.60	1.30	
H4	1.40	1.00	0.90	1.30	1.10	
H5	1.20	0.90	0.80	1.10	1.00	
H6	1.00	0.70	0.70	0.90	0.80	
H7	0.90	0.60	0.60	0.80	0.70	
DR 1-2	0.015927	0.000000	0.022769	0.029005	0.027341	
DR 2-3	0.027341	0.026578	0.026578	0.035492	0.033029	
DR 3-4	0.021247	0.015167	0.031921	0.033029	0.026578	
DR 4-5	0.024526	0.016766	0.018742	0.026578	0.015167	
DR 5-6	0.029005	0.039966	0.021247	0.031921	0.035492	
DR 6-7	0.016766	0.024526	0.024526	0.018742	0.021247	
						Average
Average:	**0.022469**	**0.020501**	**0.024298**	**0.029128**	**0.026476**	**0.024574**
Std. Dev:	0.004958	0.012211	0.004201	0.005445	0.006834	

	Variable Beam, 50 Hz					
	Settings: 10 mv/div and .1 sec/div					
	Divisions	**Divisions**	**Divisions**	**Divisions**	**Divisions**	
H1	2.00	2.50	2.00	3.10	2.50	
H2	1.70	2.30	1.80	2.80	2.30	
H3	1.50	1.90	1.60	2.40	1.90	
H4	1.30	1.60	1.30	1.90	1.60	
H5	1.10	1.40	1.10	1.80	1.40	
DR 1-2	0.025857	0.013269	0.016766	0.016197	0.013269	
DR 2-3	0.019916	0.030393	0.018742	0.024526	0.030393	
DR 3-4	0.022769	0.027341	0.033029	0.037155	0.027341	
DR 4-5	0.026578	0.021247	0.026578	0.008605	0.021247	
						Average
Average:	**0.023780**	**0.023063**	**0.023779**	**0.021621**	**0.023063**	**0.023061**
Std. Dev:	0.002650	0.006543	0.006480	0.010590	0.006543	

Table 6. Damping Ratio Calculations Using Equation 24.

	Variable Beam, 9.5 Hz						Fixed Beam, 14.3 Hz		
	Trial Number	N	Damping Ratio				Trial Number	N	Damping Ratio
	1	45	0.022217				1	37	0.027017
	2	45	0.022217				2	35	0.028560
	3	43	0.023250				3	39	0.025633
	4	47	0.021272				4	34	0.029399
	5	46	0.021734				5	33	0.030289
Average:		**45.2**	**0.022138**			**Average:**		**35.6**	**0.028180**
Std. Deviation:		1.483240	0.000735			Std. Deviation:		2.408319	0.001865
	Variable Beam, 20.2 Hz						Variable Beam, 50 Hz		
	Trial Number	N	Damping Ratio				Trial Number	N	Damp. Ratio
	1	42	0.023803				1	20	0.049938
	2	42	0.023803				2	23	0.043437
	3	40	0.024992				3	22	0.045408
	4	40	0.024992				4	26	0.038433
	5	41	0.024383				5	23	0.043437
Average:		**41**	**0.024395**			**Average:**		**22.8**	**0.044131**
Std. Deviation:		1.000000	0.000595			Std. Deviation:		2.167948	0.004147

Table 7. Damping Ratio Calculation Comparison For Plastic Beam.

	Plastic Beam, 16 Hz								Plastic Beam, 16 Hz					
	Setting: 50 ms/div and 20 mV/div								Settings: 50 ms/div and 20 mV/div					
	Results read from oscilloscope								Results read from TP2					
	Divisions	**Divisions**	**Divisions**	**Divisions**	**Divisions**				**Divisions**	**Divisions**	**Divisions**	**Divisions**	**Divisions**	
H1	1.40	1.50	1.60	2.00	1.90			**H1**	7.76	8.15	8.23	11.21	10.23	
H2	1.00	1.00	1.10	1.60	1.20			**H2**	5.81	5.71	6.27	9.25	6.81	
H3	0.70	0.70	0.70	1.10	0.80			**H3**	4.10	4.25	4.08	6.57	4.86	
H4	0.50	0.50	0.50	0.80	0.60			**H4**	2.88	3.03	3.10	5.10	3.64	
H5	0.30	0.40	0.40	0.60	0.40			**H5**	2.39	2.29	2.37	3.88	2.42	
DR 1-2	0.053475	0.064398	0.059529	0.035492	0.072942			**DR 1-2**	0.046011	0.056537	0.043251	0.030537	0.064630	
DR 2-3	0.056675	0.056675	0.071750	0.059529	0.064398			**DR 2-3**	0.055395	0.046947	0.068226	0.054368	0.053614	
DR 3-4	0.053475	0.053475	0.053475	0.050619	0.045738			**DR 3-4**	0.056124	0.053773	0.043677	0.040277	0.045956	
DR 4-5	0.081033	0.035492	0.035492	0.045738	0.064398			**DR 4-5**	0.029669	0.044521	0.042696	0.043473	0.064833	
						Average								**Average**
Average:	**0.061165**	**0.052510**	**0.055062**	**0.047845**	**0.061869**	**0.055690**		**Average:**	**0.046800**	**0.050445**	**0.049463**	**0.042164**	**0.057258**	**0.049226**
Std. Dev:	0.013331	0.012237	0.015099	0.010021	0.011483			**Std. Dev:**	0.012314	0.005643	0.012515	0.009822	0.009179	

Table 8. Effect of Damping Ratio On Shock Response.

9.5 Hz		Equation 24		Equation 25, TP2		Equation 25, O		Peak G's
	Actual Output G's	Peak G, SRS	DR	Peak G's	DR	Peak G, SRS	DR	DR = 0
PP 1	11.87	8.95	0.02	8.95	0.02	8.42	0.03	10.75
2	12.16	9.25	0.02	9.25	0.02	8.70	0.03	10.82
3	13.13	9.10	0.02	9.10	0.02	8.56	0.03	11.80
4	12.60	9.34	0.02	9.34	0.02	8.79	0.03	10.90
5	12.01	9.22	0.02	9.22	0.02	8.67	0.03	11.23
AVG	**12.35**	**9.17**	**0.02**	**9.17**	**0.02**	**8.63**	**0.03**	**11.10**
GP 1	13.56	19.46	0.02	19.46	0.02	18.64	0.03	23.17
14.3 Hz								
PP 1	10.72	11.48	0.03	11.06	0.06	10.92	0.07	13.08
2	12.21	10.91	0.03	10.51	0.06	10.40	0.07	12.90
3	11.53	11.93	0.03	11.48	0.06	11.35	0.07	13.60
4	11.38	11.26	0.03	10.83	0.06	10.69	0.07	12.80
5	11.64	11.11	0.03	10.68	0.06	10.56	0.07	12.94
AVG	**11.50**	**11.34**	**0.03**	**10.91**	**0.06**	**10.78**	**0.07**	**13.06**
GP 1	24.90	24.90	0.03	23.91	0.06	23.63	0.07	26.06
2	24.41	24.96	0.03	23.99	0.06	23.70	0.07	26.11
3	25.39	24.91	0.03	23.93	0.06	23.64	0.07	26.07
4	24.90	24.89	0.03	23.91	0.06	23.62	0.07	26.05
5	24.85	24.87	0.03	23.91	0.06	23.62	0.07	26.02
AVG	**24.89**	**24.91**	**0.03**	**23.93**	**0.06**	**23.64**	**0.07**	**26.06**
20.2 Hz								
PP 1	17.30	16.53	0.02	16.53	0.02	16.53	0.02	20.47
2	19.04	16.86	0.02	16.86	0.02	16.86	0.02	20.85
3	20.07	17.80	0.02	17.80	0.02	17.80	0.02	21.33
4	19.04	17.00	0.02	17.00	0.02	17.00	0.02	20.59
5	19.63	16.79	0.02	16.79	0.02	16.79	0.02	21.23
AVG	**19.02**	**17.00**	**0.02**	**17.00**	**0.02**	**17.00**	**0.02**	**20.89**
GP 1	21.64	27.45	0.02	27.45	0.02	27.45	0.02	28.81
2	21.68	27.67	0.02	27.67	0.02	27.67	0.02	28.32
3	21.82	27.82	0.02	27.82	0.02	27.82	0.02	28.54
4	21.97	27.42	0.02	27.42	0.02	27.42	0.02	28.70
5	21.71	27.93	0.02	27.93	0.02	27.93	0.02	28.31
AVG	**21.76**	**27.66**	**0.02**	**27.66**	**0.02**	**27.66**	**0.02**	**28.54**
50 Hz								
PP 1	42.77	43.56	0.04	44.83	0.02	44.83	0.02	50.05
2	47.85	43.82	0.04	45.20	0.02	45.20	0.02	49.85
3	50.57	43.66	0.04	44.97	0.02	44.97	0.02	48.80
4	49.41	43.39	0.04	44.70	0.02	44.70	0.02	49.51
5	49.80	44.34	0.04	45.76	0.02	45.76	0.02	49.95
AVG	**48.08**	**43.75**	**0.04**	**45.09**	**0.02**	**45.09**	**0.02**	**49.63**
GP 1	28.96	27.27	0.04	28.12	0.02	28.12	0.02	29.01
2	31.30	27.28	0.04	28.10	0.02	28.10	0.02	29.06
3	31.74	27.61	0.04	28.43	0.02	28.43	0.02	29.39
4	31.88	27.68	0.04	28.53	0.02	28.53	0.02	29.48
5	32.32	27.65	0.04	28.49	0.02	28.49	0.02	29.59
AVG	**31.24**	**27.50**	**0.04**	**28.33**	**0.02**	**28.33**	**0.02**	**29.31**

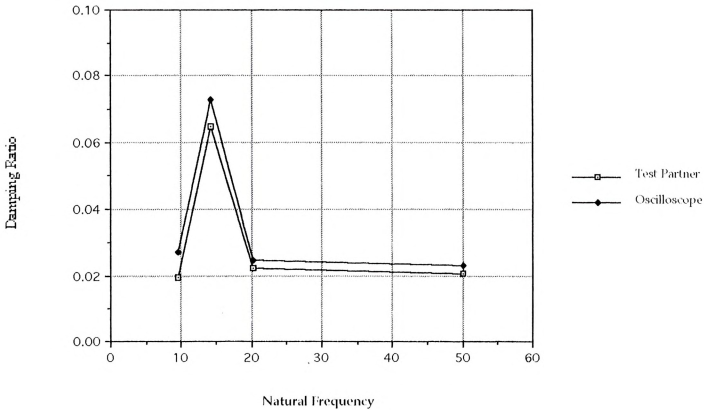

Figure 19. Damping Ratio Comparison Between Test Partner and Oscilloscope, Using Equation 25.

Damping Ratio
C:\TP2\DATA\MPD\DRB6.PL2
Channel 1

11:20:56 AM
05-24-1993

Faired Acc:		G's
Peak Acc:	23.78	G's
Min Acc:	-17.24	G's
Duration:	21.00	msec
Delta V:	155.73	In/S
Filter:	0	Hz

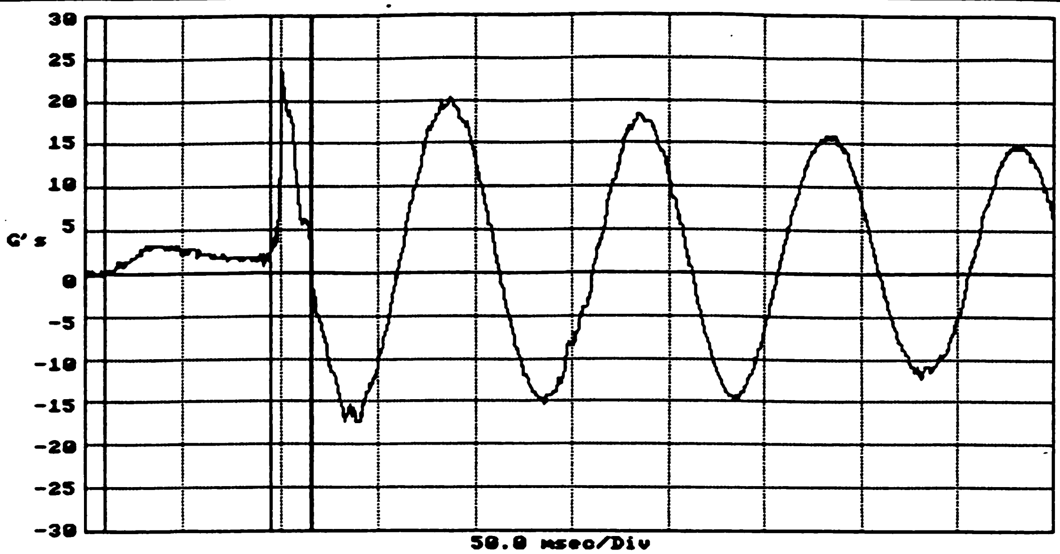

Notes: Beam has natural frequency of 9.5 Hz
Results from TP2 analysis
Damping ratio using successive peak heights, Eq. 25

Michigan State University

TEST PARTNER

Figure 20. Oscillation of Variable Beam, 9.5 Hz.

Damping Ratio
C:\TP2\DATA\MPD\DRY1.PL2
Channel 1

3:06:03 AM
04-29-1993

Faired Acc:		G's
Peak Acc:	33.11	G's
Min Acc:	-25.49	G's
Duration:	15.00	msec
Delta V:	98.99	In/S
Filter:	0	Hz

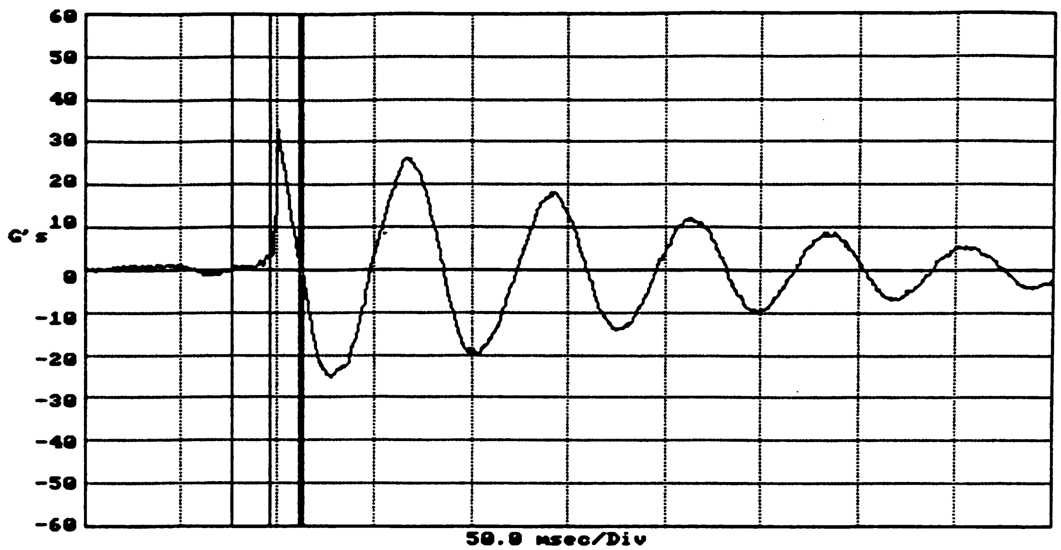

Notes: Beam has natural frequency of 14.3 Hz
Results from TP2 analysis
Damping ratio using successive peak heights, Eq. 25

Michigan State University

TEST PARTNER

Figure 21. Oscillation of Fixed Beam, 14.3 Hz.

Damping Ratio
C:\TP2\DATA\MPD\DRB1.PL2
Channel 1

3:23:22 AM
04-29-1993

Faired Acc:		G's
Peak Acc:	21.83	G's
Min Acc:	-21.63	G's
Duration:	14.00	msec
Delta V:	53.63	In/S
Filter:	0	Hz

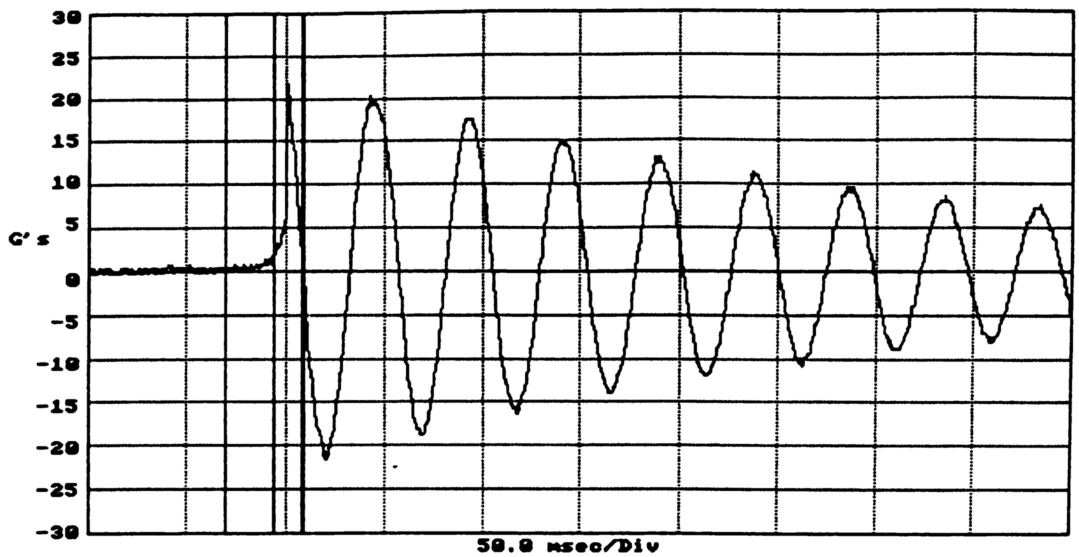

Notes: Beam has natural frequency of 20.2 Hz
Results from TP2 analysis
Damping ratio using successive peak heights, Eq. 25

Michigan State University

TEST PARTNER

Figure 22. Oscillation of Variable Beam, 20.2 Hz.

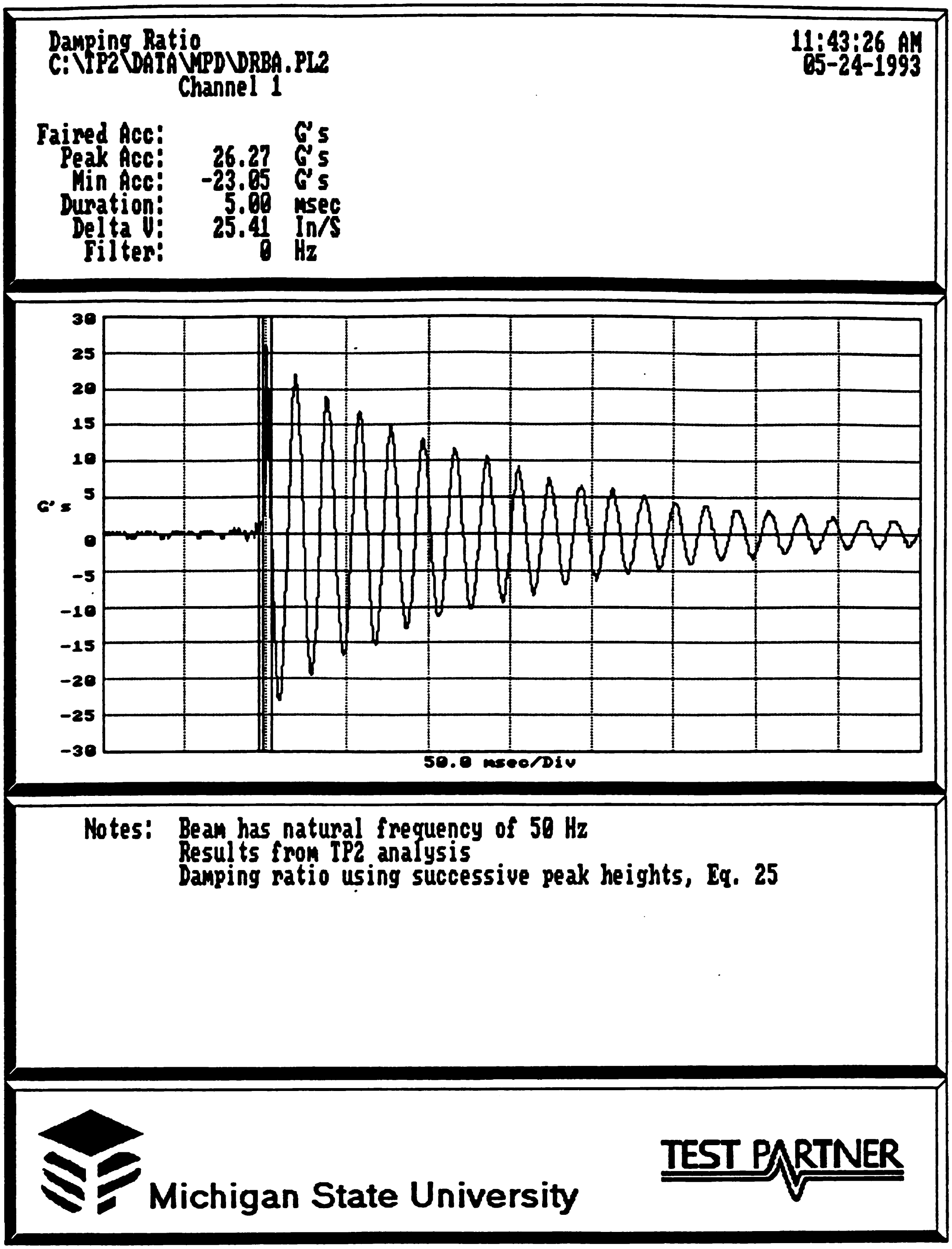

Figure 23. Oscillation of Variable Beam, 50 Hz.

SRS Evaluation, Damping Ratio
B:DRP2.PL2
Channel 1

3:39:46 PM
02-23-1993

Faired Acc:		G's
Peak Acc:	8.15	G's
Min Acc:	-6.01	G's
Duration:	12.50	msec
Delta V:	17.56	In/S
Filter:	0	Hz

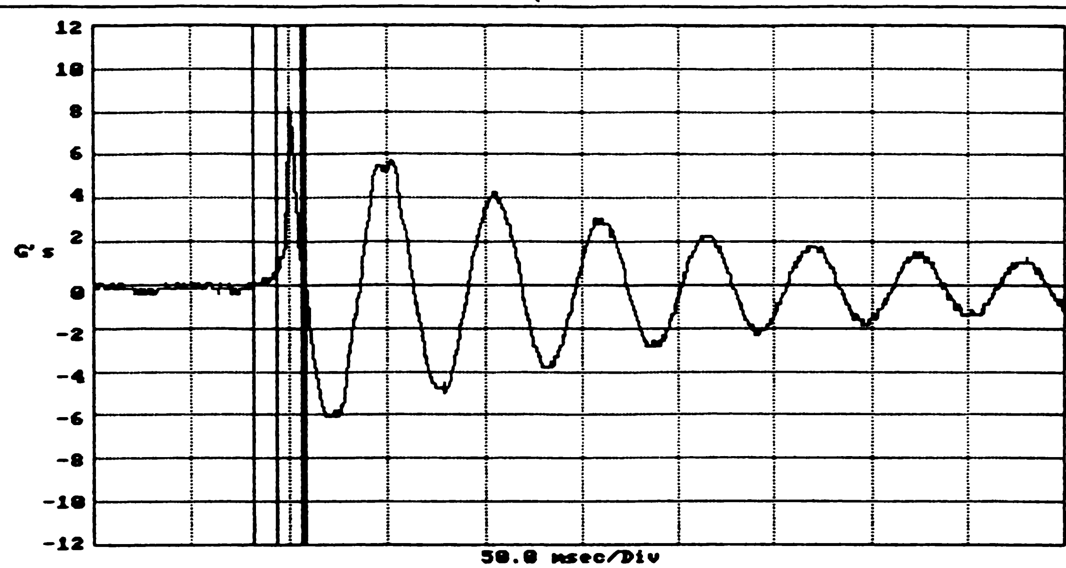

Notes: Damping ratio determined from successive peak heights using Equation 25.
Results from TP2 analysis
Plastic beam with natural frequency of 16 Hz
Peak G from first 6 heights: 8.15, 5.71, 4.25, 3.03, 2.29, 1.81

Michigan State University

TEST PARTNER

Figure 24. Oscillation of Plastic Beam, 16 Hz.

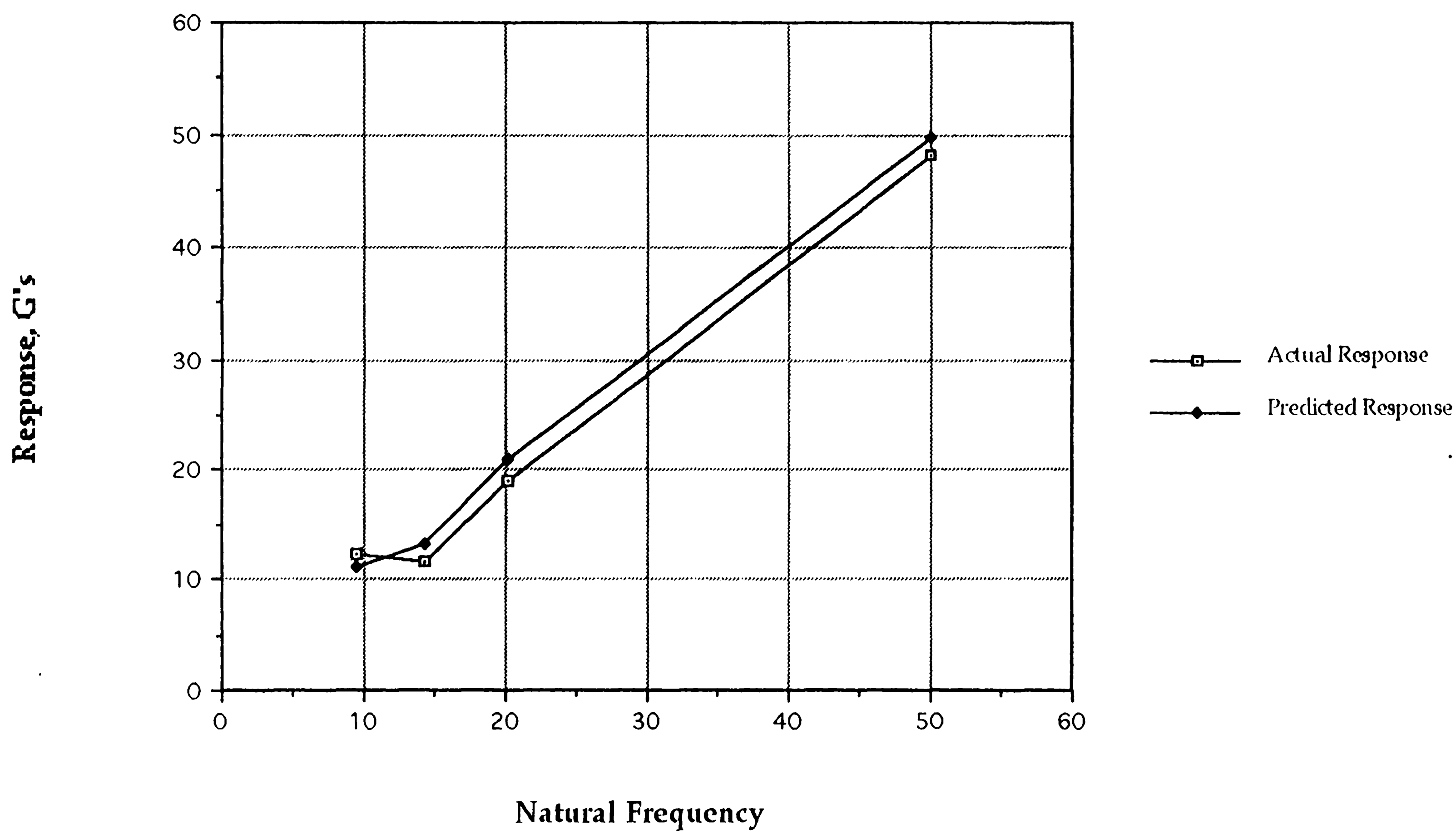

Figure 25. Comparison Between Actual and Predicted Response, 0 Damping; Plastic Programmers.

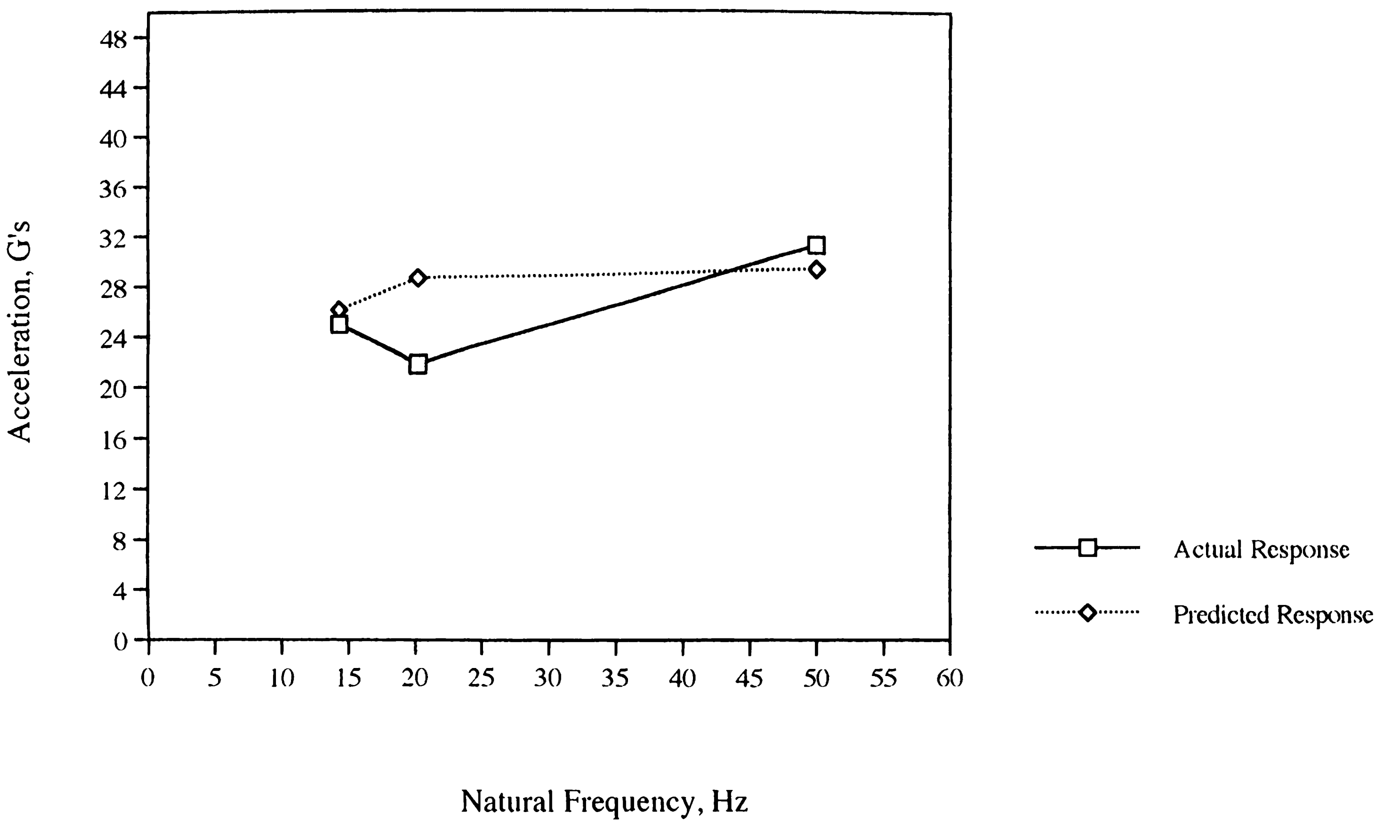

Figure 26. Comparison Between Actual and Predicted Response, 0 Damping; Gas Programmers.

APPENDIX E

APPENDIX E

The following are Figures showing the input shock, the predicted response and the actual response of the beam from the sections 4.1.2 "Results From Plastic Programmers," and 4.1.3 "Results From Gas Programmers."

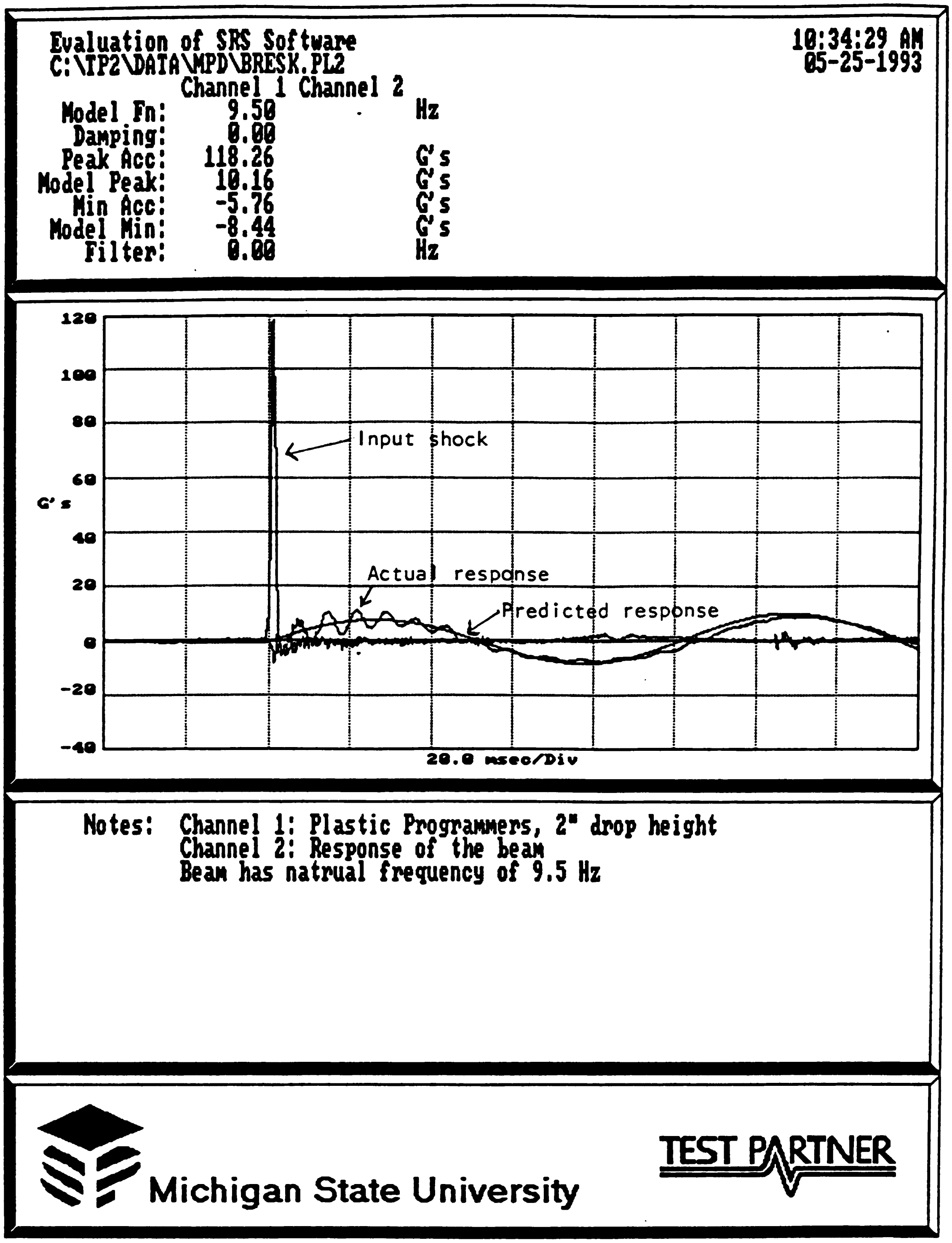

Figure 27. Actual and Predicted Response To a Plastic Programmers Drop, Variable Beam, 9.5 Hz.

Evaluation of SRS Software
C:\TP2\DATA\MPD\BRESP.PL2

11:06:01 AM
05-25-1993

	Channel 1	Channel 2	
Model Fn:	9.50		Hz
Damping:	0.00		
Peak Acc:	17.54		G's
Model Peak:	22.46		G's
Min Acc:	-7.86		G's
Model Min:	-21.84		G's
Filter:	387.60		Hz

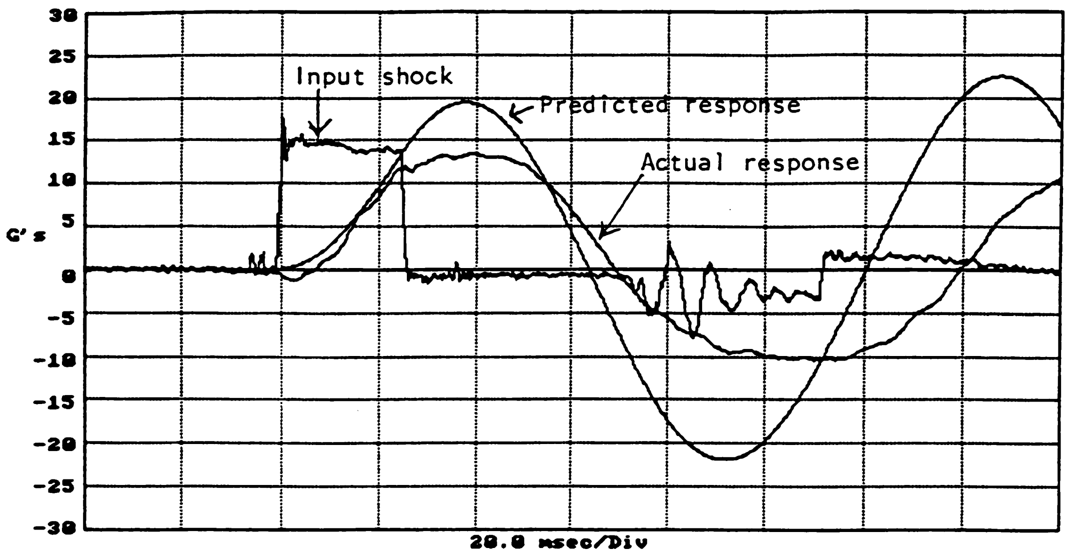

Notes: Channel 1: Gas Programmers, 8" drop, 150 psi
Channel 2: Response of beam
Beam has natural frequency of 9.5 Hz
Beam bent on this drop

Michigan State University

TEST PARTNER

Figure 28. Actual and Predicted Response To a Gas Programmers Drop, Variable Beam, 9.5 Hz.

Evaluation of SRS Software — 10:21:56 PM
C:\TP2\DATA\MPD\YRES1.PL2 — 04-29-1993

	Channel 1	Channel 2	
Model Fn:	14.30		Hz
Damping:	0.00		
Peak Acc:	77.12		G's
Model Peak:	13.03		G's
Min Acc:	-7.48		G's
Model Min:	-12.96		G's
Filter:	156.00		Hz

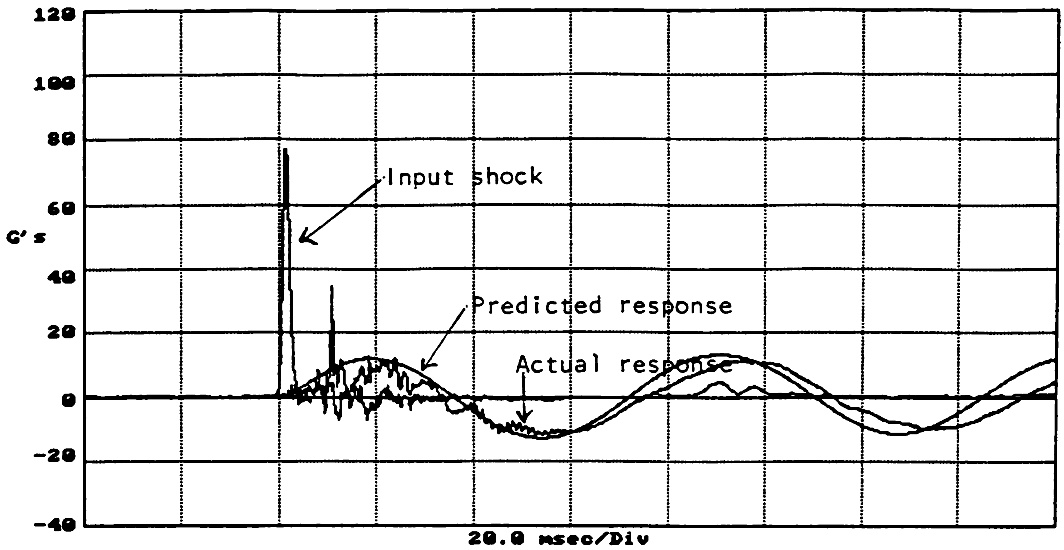

Notes: Channel 1: Plastic Programmers, 2" drop
Channel 2: Response of the beam
Beam has natural frequency of 14.3 Hz
Channel 1 is filtered to show more clearly channel 2;
channel 1 has original peak G of 118.59, which was used to calculate the shock response

Michigan State University

TEST PARTNER

Figure 29. Actual and Predicted Response To a Plastic Programmers Drop, Fixed Beam, 14.3 Hz.

Evaluation of SRS Software
C:\TP2\DATA\MPD\YRES0.PL2

10:47:35 PM
04-29-1993

	Channel 1	Channel 2	
Model Fn:	14.30		Hz
Damping:	0.00		
Peak Acc:	18.28		G's
Model Peak:	26.02		G's
Min Acc:	-9.31		G's
Model Min:	-27.43		G's
Filter:	384.62		Hz

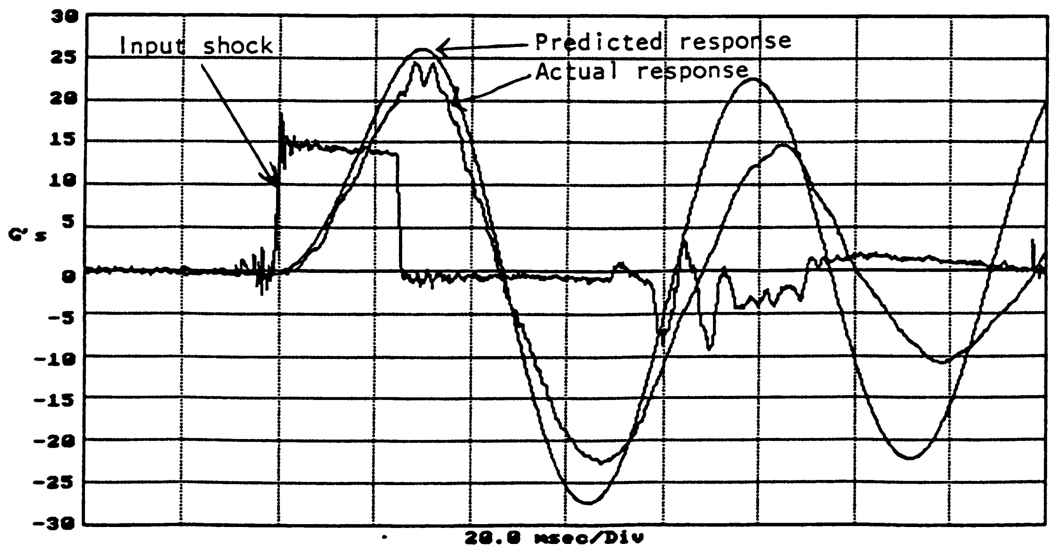

Notes: Fixed beam with natural frequency of 14.3 Hz
Channel 1: Gas Programmer, 8" drop
Channel 2: Response of C.E.
150 psi

Michigan State University

TEST PARTNER

Figure 30. Actual and Predicted Response To a Gas Programmers Drop, Fixed Beam, 14.3 Hz.

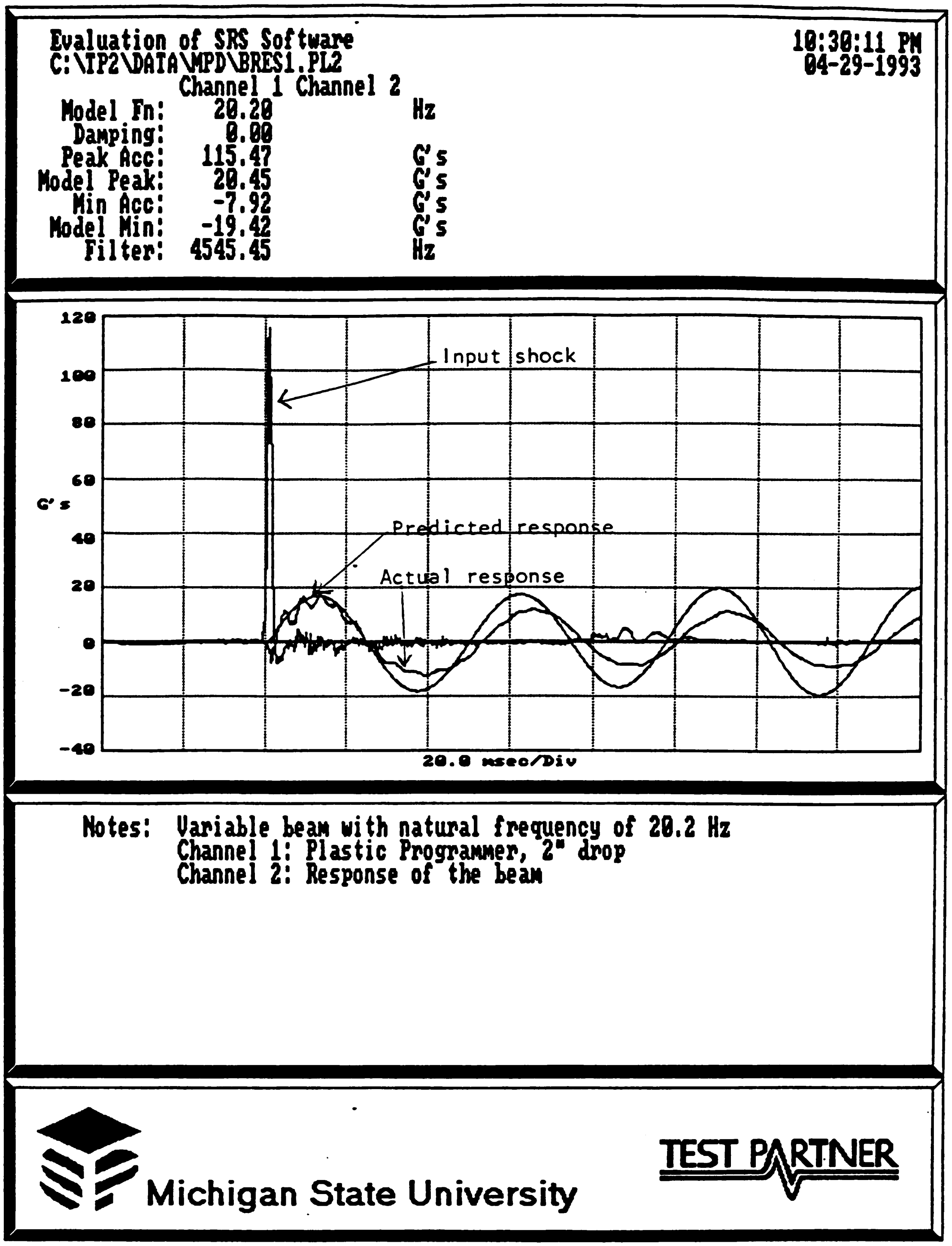

Figure 31. Actual and Predicted Response To a Plastic Programmers Drop, Variable Beam, 20.2 Hz.

Evaluation of SRS Software
C:\TP2\DATA\MPD\ND.PL2

3:33:01 PM
09-01-1993

	Channel 1	Channel 2	
Model Fn:	20.20		Hz
Damping:	0.00		
Peak Acc:	19.33		G's
Model Peak:	28.32		G's
Min Acc:	-3.63		G's
Model Min:	-30.40		G's
Filter:	367.65		Hz

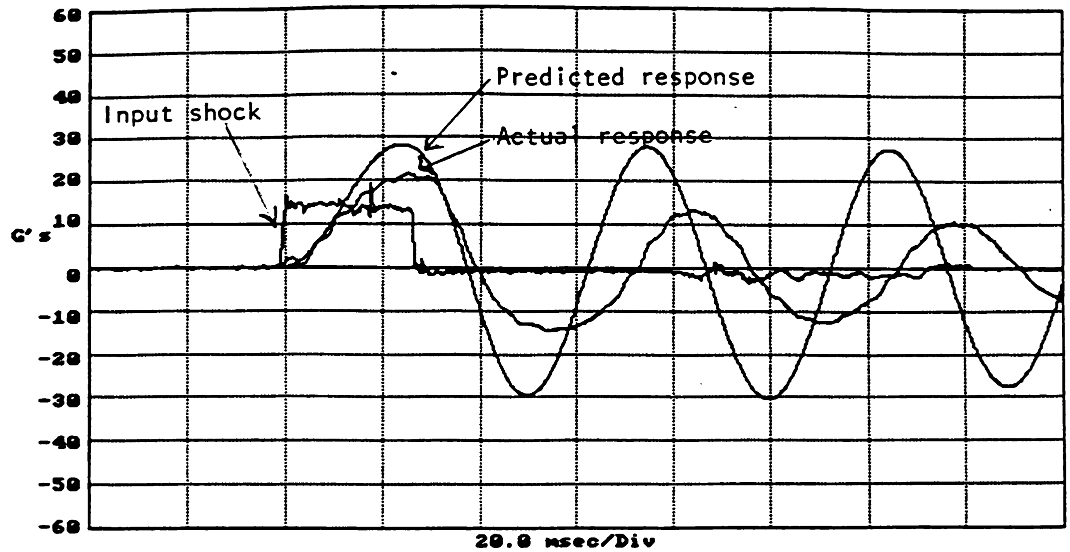

Notes: Variable beam with natural frequency of 20.2 Hz
Channel 1: Gas Programmer, 8" drop
Channel 2: Response of the beam
150 psi

Michigan State University

TEST PARTNER

Figure 32. Actual and Predicted Response To a Gas Programmers Drop, Variable Beam, 20.2 Hz.

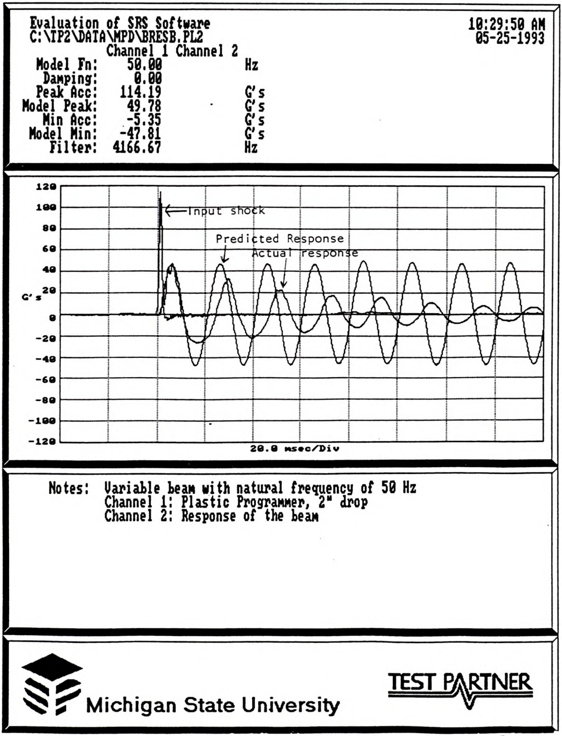

Figure 33. Actual and Predicted Response To a Plastic Programmers Drop, Variable Beam, 50 Hz.

Evaluation of SRS Software
C:\TP2\DATA\MPD\BRESF.PL2

10:59:17 AM
05-25-1993

	Channel 1	Channel 2	
Model Fn:	50.00		Hz
Damping:	0.00		
Peak Acc:	17.75		G's
Model Peak:	29.04		G's
Min Acc:	-6.69		G's
Model Min:	-26.13		G's
Filter:	373.13		Hz

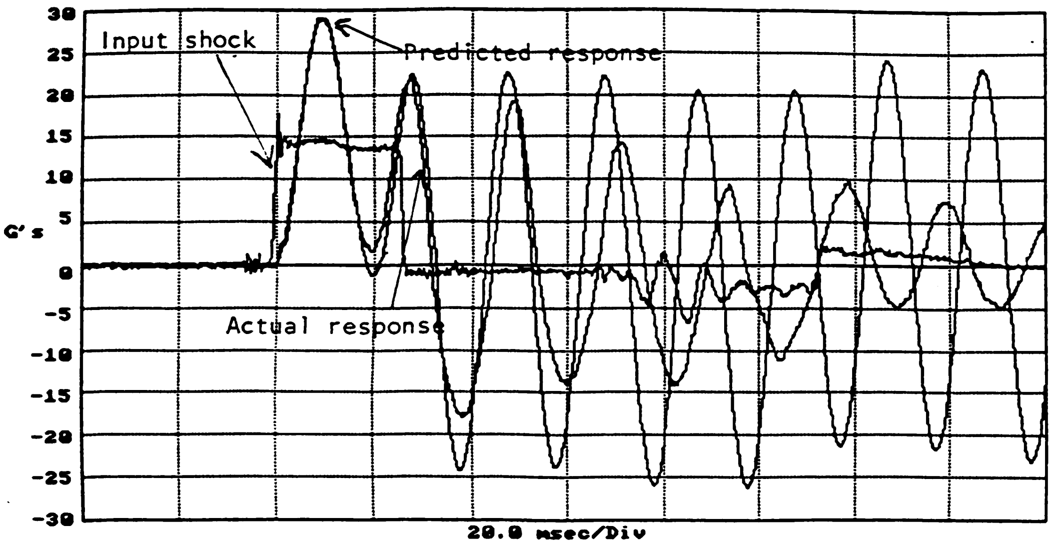

Notes: Variable beam with natural frequency of 50 Hz
Channel 1: Gas Programmer, 8" drop, 150 psi
Channel 2: Response of the beam

Michigan State University

TEST PARTNER

Figure 34. Actual and Predicted Response To a Gas Programmers Drop, Variable Beam, 50 Hz.

APPENDIX F

APPENDIX F

The following are original pulses that broke the plastic beam from the section 4.1.5 "Results From Fragility Testing." The corresponding SRS plots are Figures 15 to 18.

Michigan State University

TEST PARTNER

Evaluation of SRS Software
C:\TP2\DATA\MPD\DB4.PL2
Channel 1

12:43:28 PM
05-25-1993

Faired Acc:		G's
Peak Acc:	23.76	G's
Min Acc:	-11.83	G's
Duration:	38.60	msec
Delta V:	285.34	In/S
Filter:	262	Hz

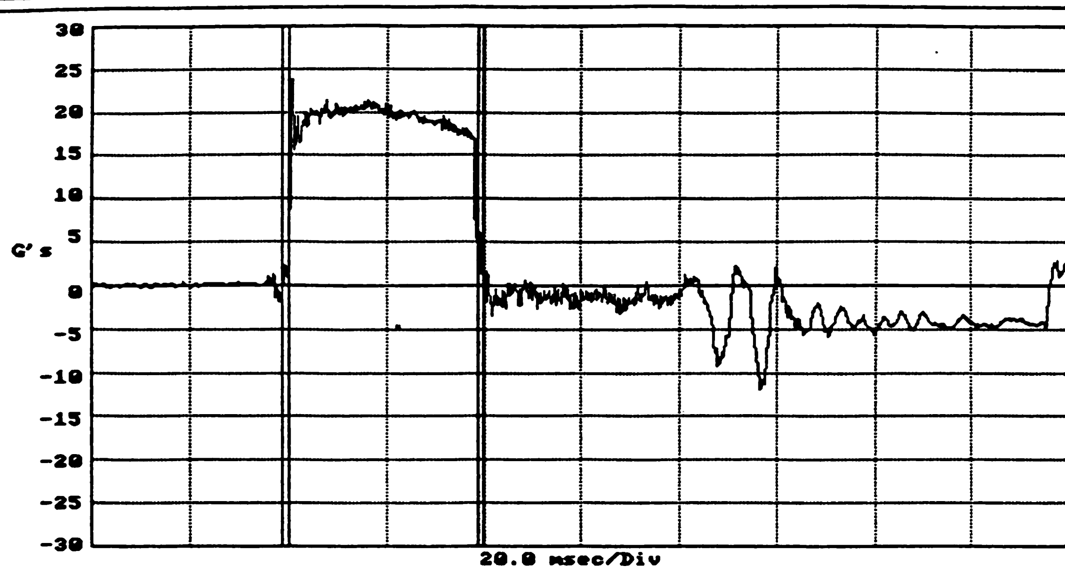

Notes: Plastic Beam
200 psi
Table Height of 30"
Beam breaks on this drop

Figure 35. 30" Gas Programmers Drop, Damage Boundary Test.

Evaluation of SRS Software
C:\TP2\DATA\MPD\DT21.PL2
Channel 1

3:34:36 PM
08-18-1993

Faired Acc:	74.56	G's
Peak Acc:	157.57	G's
Min Acc:	-139.31	G's
Duration:	15.20	msec
Delta V:	199.54	In/S
Filter:	0	Hz

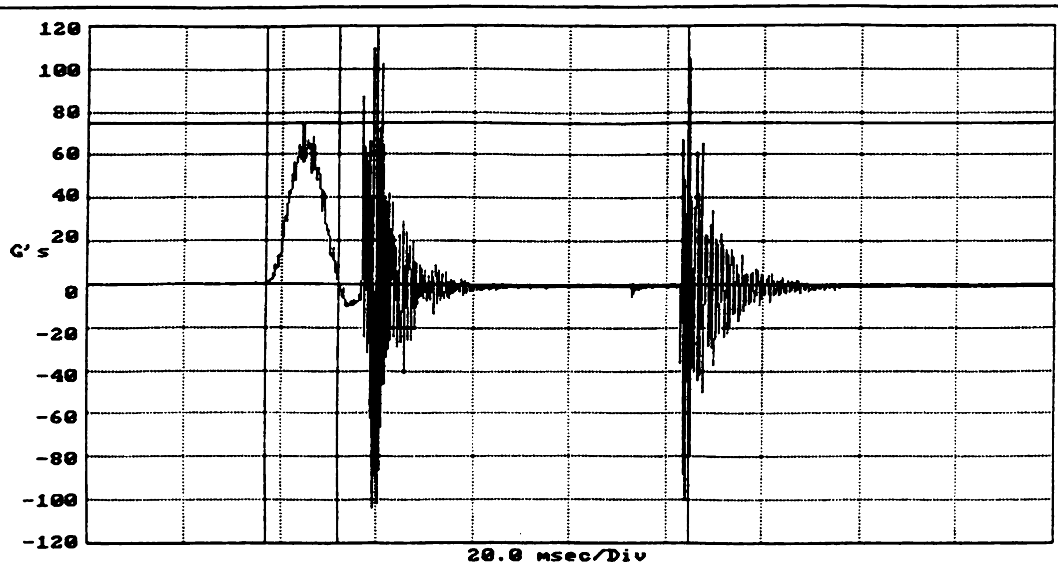

Notes: Free fall drop test
23 inches
Damage
Ethafoam 220
Plastic beam has natural frequency of 16 Hz

Michigan State University

TEST PARTNER

Figure 36. 23" Free Fall Drop Test Onto Ethafoam 220.

Michigan State University

TEST PARTNER

SRS and Damage Boundary
C:\TP2\DATA\MPD\DB2.PL2
Channel 1

12:08:09 PM
05-25-1993

Faired Acc:		G's
Peak Acc:	419.04	G's
Min Acc:	-60.94	G's
Duration:	1.80	msec
Delta V:	171.56	In/S
Filter:	0	Hz

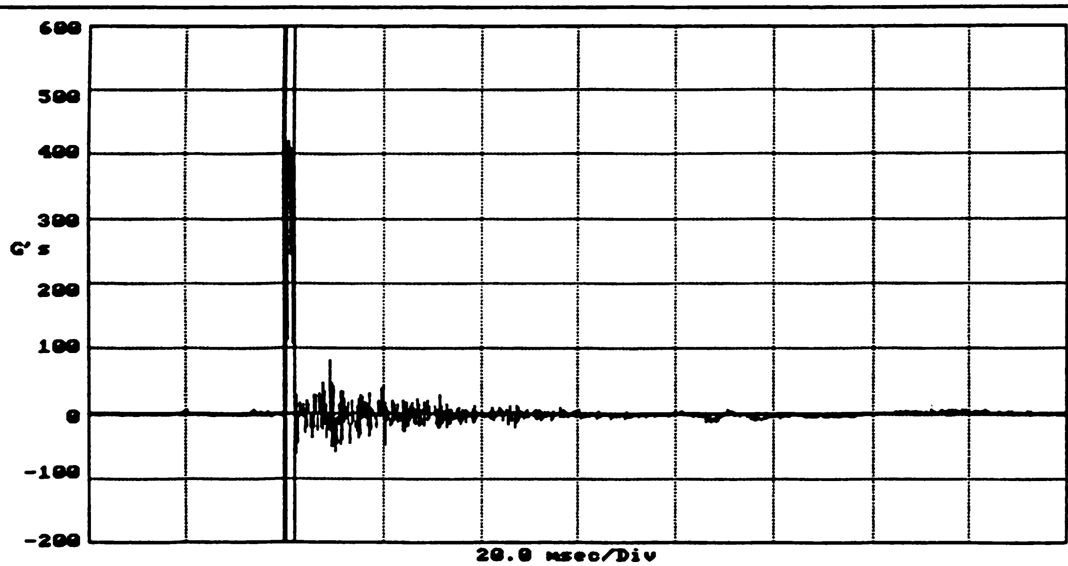

Notes: Plastic Beam #1
Plastic Programmers, 17" drop height
Beam breaks on this pulse

Figure 37. 17" Plastic Programmers Drop, Damage Boundary Test.

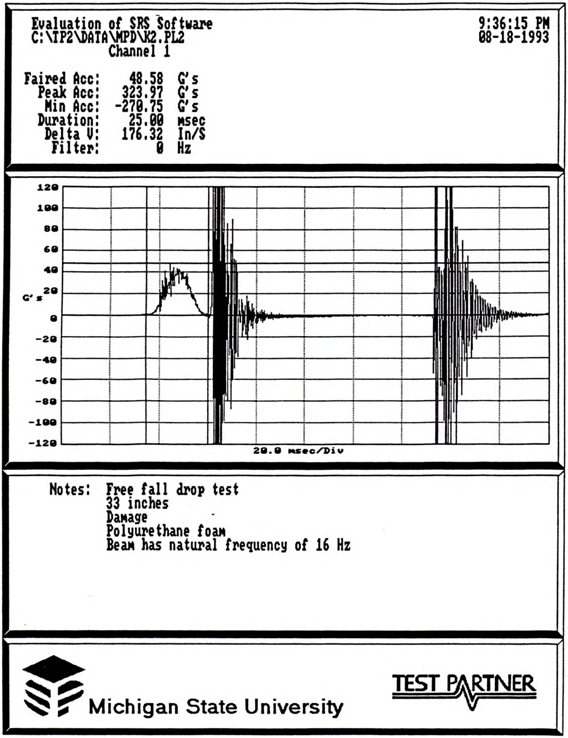

Figure 38. 33" Free Fall Drop Test Onto Polyurethane Foam.

APPENDIX G

APPENDIX G

The following is the derivation for incorporating damping ratio into the deflection failure criteria.

Recall Equation 38, which can be rewritten as

$$\frac{W}{g}\cdot\frac{d^2y}{dt^2}-c\left(\frac{dx}{dt}-\frac{dt}{dt}\right)+k(x-y) \qquad \text{Eq. 48.}$$

where: x-y = deflection of mass relative to its base

and $\frac{dx}{dt}-\frac{dy}{dt}$ = velocity of the mass relative to the base.

At maximum relative deflection, where (x-y) = d, the relative velocity is zero, and the peak deceleration of the mass becomes:

$$\frac{d^2y}{dt^2}=\frac{kgd}{W} \qquad \text{Eq. 49.}$$

Using the relations

$$G=\frac{1}{g}\cdot\frac{d^2y}{dt^2} \qquad \text{Eq. 50.}$$

and $$\frac{kg}{W}=\frac{(2\pi f_n)^2}{1-DR^2} \qquad \text{Eq. 51.}$$

where DR = damping ratio.

Substituting into Equation 49 yields:

$$\text{peak G}=\frac{(2\pi f_n)^2 d}{g(1-DR^2)} \qquad \text{Eq. 52.}$$

REFERENCES

REFERENCES

1. Greenfield, J.F. "Dealing With the Shock Environment Using the Shock Response Spectrum Analysis." Journal of the Society of Environmental Engineers. Sep. 1977 pp 3-15.

2. ASTM D332-77 (1983). "Standard Test Methods for Mechanical Shock Shock Fragility of Products Using Shock Machines."

3. Henderson, George. "Improved Protective Package Drop Test Data Analysis." IBM Annual Shock and Vibration Seminar. Boca Raton, Florida. IBM, 19 Oct. 1990.

4. Burgess, Gary. Lecture notes, Advanced Packaging Dynamics. East Lansing, Michigan State University.

5. Leinberger, David A. "Study of SRS for Product/Package Testing." Unpublished Report. East Lansing, Michigan State University. June, 1992.

6. Henderson, George. "Advanced Techniques For Shock and Vibration Analysis As Applied To Distribution Engineering." Fall 1991 IOPP P2C2 Boston Meeting, IBM Corporation Shock and Vibration Seminars, 1987, '88, '89, '90, and '91, Distribution Dynamics Labs Advanced Shock and Vibration Seminars, 1991.

7. Yang, Robert C. and Herbert R. Saffill. Development Of A Waveform Synthesis Technique - A Supplement To Response Spectrum As A Definition Of Shock Environment. Shock and Vibration Bulletin No. 42, Part 2, NRL Jan. 1972.

8. Smallwood, David O. "An Improved Recursive Formula For Calculating Shock Response Spectra." Shock and Vibration Bulletin No. 51, Part 2, pp211-216, May 1981.

9. Harris, Cyril M. Shock and Vibration Handbook. 3rd ed. New York: McGraw-Hill, 1988.

10. Keller, A.C., B.G. Pollard and E.A. Andress. Shock Spectrum Analysis And Structural Design. San Diego: Spectral Dynamics Corporation, 1973.

11. Schwartz, H.B.. and J. Santos. Shock Response Spectrum (SRS): Analysis, Interpretation and Application. Poughkeepsie: IBM Technical Report, 1989.

12. Henderson, George. Standardization of Shock Machines Using SRS Analysis. San Pedro: GHI Systems, Incorporated, 1988.

13. Tustin, Wayne, George M. Heiber, et al. Understanding And Measuring The Shock Response Spectrum. San Diego: Spectral Dynamics Corporation, 1975.

14. Newton, Robert E. "Fragility Assessment Theory and Test Procedure." U.S. Naval Postgraduate School.

15. Brandenburg, Richard K., and Julian June-Ling Lee. Fundamentals of Packaging Dynamics. Minneapolis: MTS Systems Corporation, 1985.

16. Ince, E.L. Ordinary Differential Equations. New York: Dover Publications, 1944.

17. ASTM D999-75. "Standard Methods for Vibration Testing of Shipping Containers."

MICHIGAN STATE UNIV. LIBRARIES
31293010221913